Institutionen för systemteknik
Department of Electrical Engineering

Examensarbete

Attenuation of Harmonic Distortion in Loudspeakers Using Non-linear Control

Examensarbete utfört i Reglerteknik
vid Tekniska högskolan vid Linköpings universitet
av

Marcus Arvidsson and Daniel Karlsson

LiTH-ISY-EX--12/4579--SE

Linköping 2012

LINKÖPINGS UNIVERSITET

Linköpings universitet
TEKNISKA HÖGSKOLAN

Department of Electrical Engineering
Linköpings universitet
SE-581 83 Linköping, Sweden

Linköpings tekniska högskola
Linköpings universitet
581 83 Linköping

Attenuation of Harmonic Distortion in Loudspeakers Using Non-linear Control

Examensarbete utfört i Reglerteknik
vid Tekniska högskolan vid Linköpings universitet
av

Marcus Arvidsson and Daniel Karlsson

LiTH-ISY-EX--12/4579--SE

Handledare: **Ylva Jung**
ISY, Linköpings universitet
Pär Gunnars Risberg
Actiwave AB

Examinator: **Ph.D. Martin Enqvist**
ISY, Linköpings universitet

Linköping, 7 juni 2012

Avdelning, Institution Division, Department Institutionen för systemteknik Department of Electrical Engineering SE-581 83 Linköping	**Datum** Date 2012-06-07

Språk Language	**Rapporttyp** Report category	**ISBN**
☐ Svenska/Swedish	☐ Licentiatavhandling	—
☒ Engelska/English	☒ Examensarbete	**ISRN** LiTH-ISY-EX--12/4579--SE
	☐ C-uppsats	**Serietitel och serienummer** Title of series, numbering
	☐ D-uppsats	**ISSN** —
☐ ______	☐ Övrig rapport	
	☐ ______	

URL för elektronisk version

http://www.ep.liu.se

Titel
Title

Olinjär reglering för dämpning av harmonisk distorsion i högtalare

Attenuation of Harmonic Distortion in Loudspeakers Using Non-linear Control

Författare
Author

Marcus Arvidsson and Daniel Karlsson

Sammanfattning
Abstract

The first loudspeaker was invented almost 150 years ago and even though much has changed regarding the manufacturing, the main idea is still the same. To produce clean sound, modern loudspeaker consist of expensive materials that often need advanced manufacturing equipment. The relatively newly established company Actiwave AB uses digital signal processing to enhance the audio for loudspeakers with poor acoustic properties. Their algorithms concentrate on attenuating the linear distortion but there is no compensation for the loudspeakers' non-linear distortion, such as harmonic distortion.

To attenuate the harmonic distortion, this thesis presents controllers based on exact input-output linearisation. This type of controller needs an accurate model of the system. A loudspeaker model has been derived based on the LR-2 model, an extension of the more common Thiele-Small model.

A controller based on exact input-output linearisation also needs full state feedback, but since feedback risk being expensive, state estimators were used. The state estimators were based on feed-forward or observers using the extended Kalman filter or the unscented Kalman filter. A combination of feed-forward state estimation and a PID controller were designed as well.

In simulations, the total harmonic distortion was attenuated for all controllers up to 180 Hz. The simulations also showed that the controllers are sensitive to inaccurate parameter values in the loudspeaker model. During real-life experiments, the controllers needed to be extended with a model of the used amplifier to function properly. The controllers that were able to attenuate the harmonic distortion were the two methods using feed-forward state estimation. Both controllers showed improvement compared to the uncontrolled case for frequencies up to 40 Hz.

Nyckelord
Keywords

EKF, exact linearisation, feed-forward, loudspeaker modelling, non-linear control, UKF

Abstract

The first loudspeaker was invented almost 150 years ago and even though much has changed regarding the manufacturing, the main idea is still the same. To produce clean sound, modern loudspeaker consist of expensive materials that often need advanced manufacturing equipment. The relatively newly established company Actiwave AB uses digital signal processing to enhance the audio for loudspeakers with poor acoustic properties. Their algorithms concentrate on attenuating the linear distortion but there is no compensation for the loudspeakers' non-linear distortion, such as harmonic distortion.

To attenuate the harmonic distortion, this thesis presents controllers based on exact input-output linearisation. This type of controller needs an accurate model of the system. A loudspeaker model has been derived based on the LR-2 model, an extension of the more common Thiele-Small model.

A controller based on exact input-output linearisation also needs full state feedback, but since feedback risk being expensive, state estimators were used. The state estimators were based on feed-forward or observers using the extended Kalman filter or the unscented Kalman filter. A combination of feed-forward state estimation and a PID controller were designed as well.

In simulations, the total harmonic distortion was attenuated for all controllers up to 180 Hz. The simulations also showed that the controllers are sensitive to inaccurate parameter values in the loudspeaker model. During real-life experiments, the controllers needed to be extended with a model of the used amplifier to function properly. The controllers that were able to attenuate the harmonic distortion were the two methods using feed-forward state estimation. Both controllers showed improvement compared to the uncontrolled case for frequencies up to 40 Hz.

Sammanfattning

Högtalaren uppfanns för nästan 150 år sedan och trots att mycket av tillverkningen har ändrats är grundtanken fortfarande samma som då. För att kunna återskapa ett rent ljud består moderna högtalare av dyra material som ofta kräver avancerad tillverkningsutrustning. Det relativt nystartade företaget Actiwave AB använder digital signalbehandling för att kompensera för högtalare med dåliga akustiska egenskaper. Deras metoder kompenserar i nuläget endast för högtalarens linjära distorsion men ingen kompensering görs för den olinjära distorsionen, så som harmonisk distorsion.

För att kunna dämpa den harmoniska distorsionen har det här examensarbetet tagit fram regulatorer baserade på exakt linjärisering. Denna typ av reglering kräver en god modell av systemet. Därför har en högtalarmodell tagits fram, utgående från LR-2-modellen, som är baserad på den vanliga Thiele-Small-modellen.

En regulator som använder exakt linjärisering behöver även full tillståndsåterkoppling. Eftersom återkoppling riskerar att kräva dyra sensorer har metoder för tillståndsskatttning använts. Skattningarna använde sig av antingen framkoppling eller observatörer med olinjära Kalmanfilter. En kombination av framkoppling och återkoppling med en PID-regulator har även tagits fram.

I simuleringar dämpades den totala harmoniska distorsionen för frekvensinnehåll upp till 180 Hz. Simuleringarna visade också att regulatorerna är känsliga för fel hos högtalarmodellens parametervärden. För fysiska experiment behövde systemet utökas med en modell av den använda förstärkaren för att fungera. Med den modifikationen lyckades de två regulatorerna som använde framkoppling för att skatta tillstånden, att dämpa den harmoniska distorsionen för frekvenser upp till 40 Hz.

Acknowledgements

Even though most of the work were done by ourselves, there are some people that deserve a token of gratitude.

First, we would like to thank Actiwave and supervisor Pär Gunnars Risberg for making this thesis possible. It has been great loads of fun between the agonies.

Thanks to our examiner Ph.D. Martin Enqvist for your support and your, seemingly inhuman, ability to give a satisfactory answer to almost every question we have had.

Huge thanks to Ylva Jung for your help with everything, from finding ancient, yet functional, power sources to proof-reading this report.

We would also like to thank the support staff at ISY, and especially Jean-Jaques Moulis, for a great deal of help with the laboratory equipment.

Great thanks to our families. Without your love and support none of this would have been possible.

Special thanks to Karl-Johan Barsk, Jacob Bernhard and Patrik Johansson for motivational 'fika'-breaks and good sportsmanship when beaten in badminton. Call whenever you want a rematch.

Daniel would also like to thank Cissi for everything she has put up with during this work, you are the best!

All those we have not mentioned, you are all equally unimpo... ehh... important to us. We would love to get back together for a 'fika' someday.

Aliquando et insanire iucundum est
Linköping, June 2012
Marcus Arvidsson and Daniel Karlsson

Contents

Notation

Loudspeaker

u	Voltage at speaker terminals	[V]
i	Terminal current	[A]
x	Cone displacement	[m]
$\dot{x}$	Velocity of the cone movement	[m/s]
R_e	Voice coil resistance (DC)	[Ω]
L_e	Voice coil inductance	[H]
R_2	Eddy current resistance	[Ω]
L_2	Parainductance	[H]
i_2	Current flowing through L_2	[A]
Bl	Force factor	[Tm]
C_{ms}	Suspension compliance	[m/N]
R_{ms}	Suspension mechanical resistance	[Ω]
F_m	Reluctance force	[N]
M_{ms}	Diaphragm mechanical mass	[kg]
M	Diaphragm mechanical mass + air load	[kg]
$\mathbf{x}$	State vector	
x_1	Movement of coil, first state (x)	[m]
x_2	Velocity of coil, second state ($\dot{x}$)	[m/s]
x_3	Terminal current, third state (i)	[A]
x_4	Corrent through L_2, fourth state (i_2)	[A]

AC amplifier

u_{amp}	Voltage distortion	[V]
τ	Time constant	[s]
u	Input signal	[V]
e	Output to loudspeaker	[V]
V_{amp}	Amplification constant	

Controller

LD	Linear dynamics	
ID	Inverse dynamics	
w	Signal source	[V]
v	Linear dynamics control signal	[V]
u	Inverse dynamics control signal	[V]
$\hat{\mathbf{x}}$	Estimated state vector	
$\mathbf{z}$	Transformed state vector	
α	Amplifier constant	

Observer

EKF	Extended Kalman filter
EKF2	Second-order Extended Kalman filter
UKF	Unscented Kalman filter
AUKF	Augmented Unscented Kalman filter
$\mathbf{K}$	Kalman gain vector
$\mathbf{Q}$	Covariance matrix for the process noise
$\mathbf{R}$	Covariance matrix for the measurement noise

Distortion

HD	Harmonic distortion
IMD	Intermodulation distortion
THD	Total harmonic distortion

Part I

Background

1
Introduction

The first loudspeaker was invented almost 150 years ago and even though much has changed regarding the manufacturing and what materials they consist of, the main idea is still the same. The main purpose is to have the loudspeaker create sound according to its input without adding any distortion. The problem with distortion has mainly been approached by experimenting with different materials in the loudspeaker. Because of the high material cost of making a high fidelity loudspeaker, it is desirable to explore other ways of reducing the unwanted distortion. To achieve this, a better understanding of where the distortion is generated is needed and this can be obtained by creating accurate models of the loudspeaker. However, this is no simple task and some of the most difficult parts when creating a model of a loudspeaker is that it is non-linear and consists of many parameters that are affected by non-linearities caused by factors such as material, frequency and temperature. Even when a decent model of a speaker is available, the manufacturer still needs to make a trade-off between fidelity, size and cost.

One way of approaching this problem without building the speaker out of expensive materials is to use digital signal processing. Since a linear and time-invariant system retains the frequency of the input, one way of reducing the distortion is to try to eliminate the non-linearities and get a linear input-output problem. By using digital signal processing it is, at least in theory, possible to compensate for the distortion by using an accurate model of the loudspeaker. The compensation can be done in multiple ways and this thesis will explore the possibilities to create a working control law that gives satisfactory results in practice.

The work has been made in collaboration with Actiwave AB and has been based on the previous findings of Jakobsson and Larsson [2010]. Actiwave AB spe-

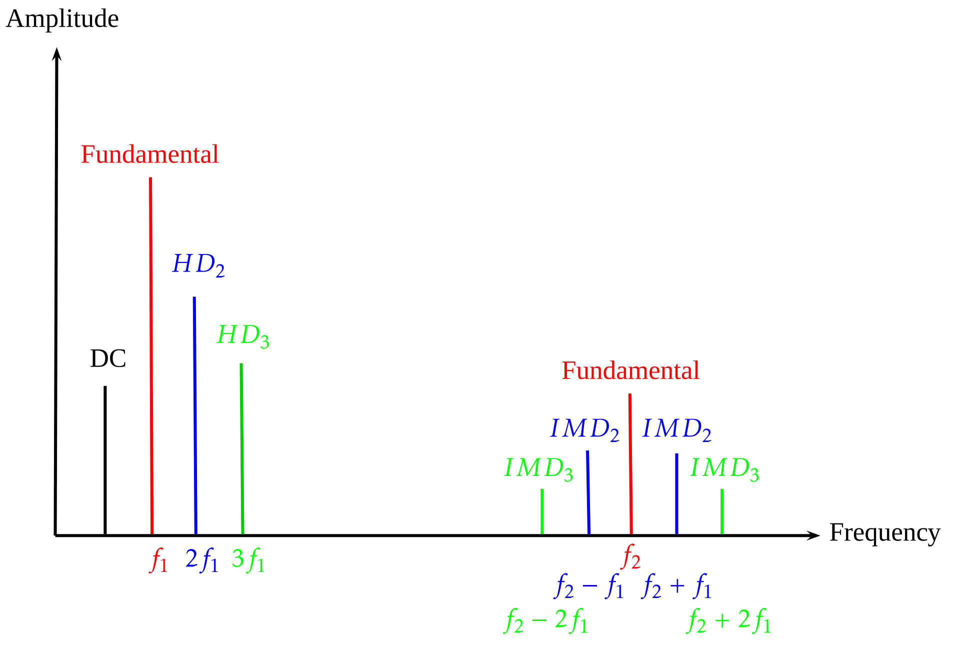

Figure 1.1: *Harmonic and intermodulation distortion for two fundamental frequencies.*

cialises in digital signal processing for audio applications and is the developer of the loudspeaker brand Opalum. Their headquarters are situated in Solna, Sweden.

1.1 Purpose

An ordinary loudspeaker behaves in different ways when fed with signals of different frequencies and amplitude. For example, the cone excursion is heavily dependent on the input because a large input amplitude means a high sound and thereby requires the loudspeaker to move more air than if the amplitude would have been smaller. This means that the output and thus the non-linearities depend on the input and have greater impact when playing at higher amplitudes.

There are two main types of loudspeaker distortion, called harmonic distortion (HD) and intermodulation distortion (IMD) [Boer et al., 1998]. Humans are in some way used to HD, since the ear itself actually creates harmonic distortion if the sound pressure is high enough. Intermodulation distortion is less enjoyable to listen to, and appears as frequency components at the frequencies calculated as the differences between, and sums of, the fundamental frequencies and harmonics. This means that if the harmonic distortion is attenuated, the intermodulation distortion will be attenuated.

Figure 1.1 on the facing page shows the distortion of two sinusoidal signals with different frequencies which results in both harmonic and intermodulation distortion. A piece of music often consists of a higher number of fundamental frequencies than two so this is not a very common case. The example works however well to illustrate the different types of distortion.

A reasonable question to raise before removing all distortion is to ask if all distortion really is bad. In one sense it is. If it is desired to enjoy music the way its creator intended it, there can be no distortion added to the signal. On the other hand, some stereo enthusiasts claim that a certain level of distortion makes the audio picture better. A good example of this is the valve amplifier. This type of amplifier does not saturate the signal with a sharp edge, but instead uses 'soft clipping' to round off the signal. The effect is illustrated in Figure 1.2, and is usually spoken of as a quite pleasurable 'smoothness' in the sound [Ballou, 2005].

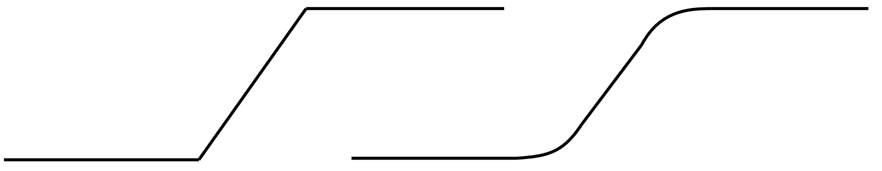

Figure 1.2: *Difference between sharp edge saturation (left) and 'soft clipping' (right).*

1.2 Limitations

During this thesis, a few limitations have been made to make it fit the time schedule. First of all, no modelling of the loudspeaker's enclosure has been made. This should be necessary to develop a functional product for the consumer market.

Another limitation is that the signals that have been used only cover relatively low frequencies. However, it is unclear how much more information that would have been added by using higher frequencies since most of the non-linearities occur when the cone excursion is large which is mainly valid for low frequencies.

The performance of a loudspeaker depends on the ambient temperature which may vary over time. This dependency has been neglected and instead the focus has been to find a functional controller for shorter runs.

Due to lack of advanced measuring equipment, the loudspeaker's internal parameters have not been determined exactly. Instead, a method of estimating the parameter values from measured impedance has been used.

1.3 Approach

Approximately the same task was investigated in Jakobsson and Larsson [2010] and they used a controller based on exact input-output linearisation with feed-forward or observer-based state estimation. Even though they could show satisfactory simulation results, an implementation of the feed-forward controller showed no improvement to the uncontrolled case. Hence, the first step was to redo the calculations done in Jakobsson and Larsson [2010] and try to figure out why the compensation failed in practice.

To ensure that the exact input-output linearisation was a suitable approach, the controller based upon it was evaluated in simulation for different levels of process noise. Additionally, observer-based estimators were designed based on nonlinear filtering using the extended Kalman filter and the unscented Kalman filter.

In contrast to the technically advanced methods using observers, approaches using the less complex PID controller have been made. One of these methods functions as an extension to the feed-forward case, and hence uses both the predicted states and a measurement to control the system.

The methods that were successful in simulations were implemented on a real-time processor using Matlab's xPC Target [Mathworks, 2008]. These methods were evaluated and compared using the level of total harmonic distortion.

1.4 Thesis outline

In the upcoming Chapter 2, the necessary theory for designing the controllers are described. The following Chapter 3 contains information about the loudspeaker model and how it was derived. In Chapter 4 the controllers and state estimators are designed by using theory and model work from the previous chapters. Chapter 5 and 6 consist of results from simulations and experiments, respectively. In the last part, Chapter 7 holds a discussion about the results, Chapter 8 holds the conclusions for this thesis, and in Chapter 9, some future work are proposed.

2

Theory

This chapter will provide the reader with the theoretical knowledge to understand the upcoming chapters. First, the basics of a moving-coil loudspeaker are explained. This is followed by some principles in control theory and signal processing regarding exact input-output linearisation and non-linear filtering for estimation.

2.1 Moving-coil loudspeaker

A loudspeaker is a transducer that converts electric signals to acoustic waves. There exists different types of loudspeakers like moving-coil, ribbon and electrostatic. The most common of these is the moving-coil loudspeaker and this type will be studied in this thesis. The moving-coil loudspeaker consists of a cone that is put into motion by an electrical input signal. This is done by a coil that is located in an air gap in which there is a magnetic field produced by a magnet, the coil is also attached to the input signal. When there is an input, the voltage in the signal interacts with the stationary magnetic field and creates a mechanical force. Since the magnet is fixed, the force will generate a motion of the coil and thereby the cone. The motion of the cone will produce pressure variations that manifests as sound. A cross section of a moving coil loudspeaker can be seen in Figure 2.1 on the following page.

The loudspeaker is a non-linear system and consists of several parameters and non-linear functions. Parameters that affect the non-linear behaviour are, for example, position of the cone, ageing and the temperature of the material and its surroundings. According to Bright [2002], the parameter that affects the non-linearities the most is the position of the cone, and the further away the cone is

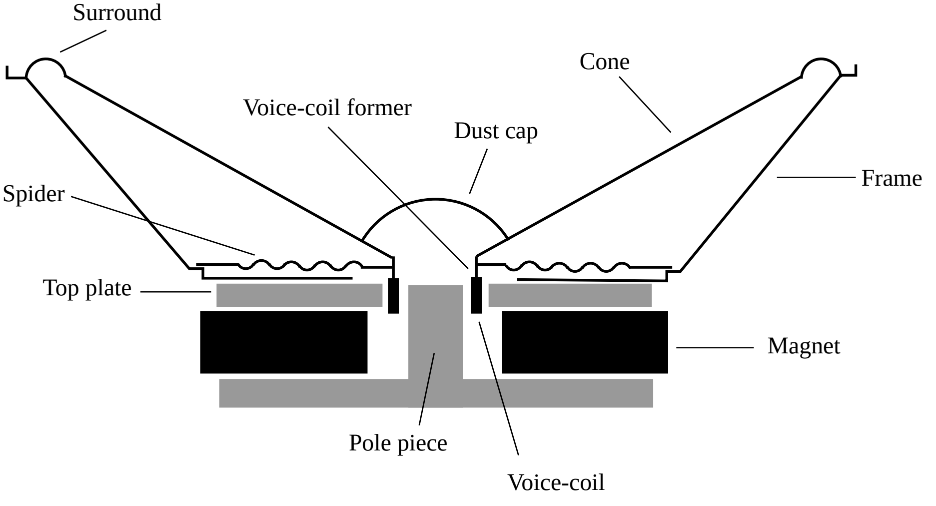

Figure 2.1: *Cross section of a loudspeaker.*

from the equilibrium, the bigger is the non-linear behaviour. If all signals are in the small signal domain the non-linearities can be neglected, but for the large signal domain they are important. According to Pedersen and Agerkvist [2008] some non-linearities will affect the system more than others and these will be discussed below.

2.1.1 Force factor

The force factor $(B \cdot l(x))$ is described in Pedersen [2008] as the power generated by the magnetic flux density, B, and the length of the voice-coil wire affected by the flux, $l(x)$. When the voice coil is moved away, the amount of wire affected by the flux density decreases and the force factor will decrease. This means that the force factor has a strong position dependency. Later in this thesis, the force factor will be denoted as the more customary $Bl(x)$.

2.1.2 Suspension compliance

The suspension in a loudspeaker has the purpose to center the voice coil at a resting position. It is created by two components, the spider and the edge suspension of the cone. The spider is usually made of polymer and the edge suspension is often made of rubber. Together with the mass of the cone and the air that it moves, the compliance decides the resonance frequency of the loudspeaker. In a linear model, the suspension is modelled as a linear spring with a viscous damping in parallel. This is only true for small displacement of the cone and for bigger ones it has been shown that it behaves non-linearly [Bright, 2002]. Pedersen [2008] mentions that the temperature is another factor that changes the behaviour of the materials, thereby also makes the compliance non-linear.

2.1.3 Voice-coil induction

The electric impedance depends on the position of the coil. This can be explained by a displacement varying inductance. The current in the voice coil generates a magnetic field that goes through magnet, iron and air. When the coil is in free air, above the gap, the inductance is lower than when the coil is below the gap where it is surrounded by steel which lowers the magnetic resistance [Klippel, 2006].

2.1.4 Other nonlinearities

There are also other non-linearities that influence the output of the loudspeaker like Doppler effect, fabrication errors and material properties [Klippel, 2006]. The Doppler effect stems from the fact that there will be different distances between the cone placement and the listening point which creates a slight phase modulation. Fabrication errors can be a loose glue joint, a wire hitting the cone or loose particles in the gap. In addition to suspension compliance, other parts that are known to change characteristics due to material properties are the voice-coil former and the dust cap.

2.2 Exact input-output linearisation

When handling non-linear systems it is a common approach to approximate the system with a linearisation around an equilibrium [Glad and Ljung, 2008]. By doing this, it is possible to control the system with linear control methods but the approach will only be valid close to the chosen equilibrium. The method can also be generalised to systems with multiple inputs and outputs as shown in Slotine and Li [1991].

Another way of handling non-linearities in systems with one input and one output is described in Glad and Ljung [2009]. Consider the following non-linear system on state-space form

$$\begin{aligned} \dot{\mathbf{x}} &= f(\mathbf{x}) + g(\mathbf{x})\,u \\ y &= h(\mathbf{x}) \end{aligned} \tag{2.1}$$

where u is the input and y is the output. The goal is to compensate for the non-linearities by generating a control law that makes the system linear. Note that the result will be a perfectly linear system and not an approximation as in the more common linearisation approach. This method is called exact input-output linearisation.

To generate a control law that linearises the system there must be a way to find out how the output depends on the input. The output, y, in (2.1) does not depend on the input, u, directly but since the input is affecting the state vector, $\mathbf{x}$, the output will be affected eventually. As described in Slotine and Li [1991] a measurement of this relation is the relative degree. A system's relative degree is equal to the number of times it is needed to take the derivative of the output before it depends explicitly on the input. In order to acquire a more mathematical relation, the notion of Lie derivatives must be explained. The Lie derivative in the direction of $f(\mathbf{x})$ is

$$L_f = f_1 \frac{\partial}{\partial x_1} + f_2 \frac{\partial}{\partial x_2} + \ldots + f_n \frac{\partial}{\partial x_n}. \tag{2.2}$$

The time derivative of y, when defined as in (2.1), can be expressed using Lie derivatives as

$$\begin{aligned} \dot{y} &= \frac{dh(\mathbf{x})}{d\mathbf{x}}\dot{\mathbf{x}} \\ &= \frac{dh(\mathbf{x})}{d\mathbf{x}} f(\mathbf{x}) + \frac{dh(\mathbf{x})}{d\mathbf{x}} g(\mathbf{x})\, u \\ &= L_f h(\mathbf{x}) + L_g h(\mathbf{x})\, u. \end{aligned} \tag{2.3}$$

From this expression, it is possible to see a connection between the relative degree, ν, and Lie derivatives. The connection can be written as

$$\begin{aligned} &\nu = 1 : L_g h \not\equiv 0 \\ &\nu = 2 : L_g h \equiv 0, L_g L_f h \not\equiv 0 \\ &\nu = 3 : L_g h \equiv 0, L_g L_f h \equiv 0, L_g L_f^2 h \not\equiv 0. \end{aligned} \tag{2.4}$$

Like in Slotine and Li [1991] this can be generalised into the definition that the relative degree, ν, of a system is the smallest positive integer such that $L_g {L_f}^{\nu-1} h$ is not equal to 0. Additionally, ν is a strong relative degree if $L_g L_f^{\nu-1} \neq 0$ everywhere. In this case the derivative of order ν for y can be written

$$y^{(\nu)} = L_f^{\nu} h + u L_g L_f^{\nu-1} h, \text{ where } L_g L_f^{\nu-1} h \neq 0\ \forall x. \tag{2.5}$$

By introducing a non-linear control law for u, there is a way to acquire a linear relation between the reference input, r, and the output according to

$$\begin{aligned} u &= \frac{1}{L_g {L_f}^{\nu-1} h}\left(r - {L_f}^{\nu} h\right) \\ y^{(\nu)} &= r. \end{aligned} \tag{2.6}$$

This will work safely for systems with the relative degree equal to the number of states. In Glad and Ljung [2009] it is shown that systems with relative degree lower than the number of states might contain internal harmful dynamics. To further investigate whether that kind of dynamics exists, it is essential to see the exact linearisation as a change of basis according to

$$\mathbf{z} = \begin{pmatrix} z_1 \\ z_2 \\ \vdots \\ z_\nu \\ z_{\nu+1} \\ \vdots \\ z_n \end{pmatrix} = \begin{pmatrix} h \\ L_f h \\ \vdots \\ L_f{}^{\nu-1} h \\ \psi_1 \\ \vdots \\ \psi_{n-\nu} \end{pmatrix}. \tag{2.7}$$

Note that ψ_i can be chosen arbitrarily for all i as long as the transformation is invertible in the sense that a unique x can be derived from a given z.

By applying the control law from (2.6), the state derivatives $\dot{z}_1, ..., \dot{z}_\nu$ will render linear equations, but the equations for $\dot{z}_{\nu+1}, ..., \dot{z}_n$ may contain non-linear dynamics that can be harmful for the system. Those dynamics are called zero dynamics and it is very important to investigate the zero dynamics of the system when designing an exact input-output linearisation since they might cause internal signals to grow unbounded and hence damage the system.

In Glad and Ljung [2009] it is stated that the zero dynamics are often controllable, if not stable, in practice and therefore allow the controller to work properly if correctly designed. If the zero dynamics still cause problems there is often a possibility to redefine the output since the controller needs full state feedback anyway. This technique will generate a totally new problem to solve, that might be without zero dynamics.

2.3 Observers

Many control designs require full state feedback. In practice it is expensive, and in some cases even impossible, to measure all states in a system. This problem requires a solution based on observers, systems that estimate all states based on the possible measurements. There are many ways to design an observer but only two common non-linear versions based upon the Kalman filter will be described here.

2.3.1 Extended Kalman filter (EKF)

A natural approach to handle non-linear systems is to linearise them and then apply linear methods. As described in Gustafsson [2010], the extended Kalman filter utilises Taylor series to linearise around the current estimate. Thanks to this fairly straightforward algorithm, the EKF has been widely used in various applications.

The most common variants of EKF are based on the first- and second-order Taylor expansions. This means that the first-order EKF only uses the Jacobian for linearisation while the second-order EKF uses the Hessian as well. With the system

$$\begin{aligned} \mathbf{x}_{k+1} &= \mathbf{f}\left(\mathbf{x}_k, u_k\right) + \mathbf{w}_k \\ \mathbf{y}_k &= \mathbf{h}\left(\mathbf{x}_k\right) + \mathbf{v}_k, \end{aligned} \tag{2.8}$$

the second-order EKF algorithm can be described through the following steps.

First a prediction step,

$$\begin{aligned} \hat{\mathbf{x}}_{k|k-1} &= \mathbf{f}\left(\hat{\mathbf{x}}_{k-1|k-1}, u_{k-1}\right) + \frac{1}{2}[\mathrm{tr}(\mathbf{f}''_{i,x}(\hat{\mathbf{x}}_{k-1|k-1})\mathbf{P}_{k-1|k-1})]_i \\ \mathbf{P}_{k|k-1} &= \mathbf{Q} + \mathbf{f}'_x(\hat{\mathbf{x}}_{k-1|k-1})\mathbf{P}_{k-1|k-1}(\mathbf{f}'_x(\hat{\mathbf{x}}_{k-1|k-1}))^T \\ &\quad + \frac{1}{2}[\mathrm{tr}(\mathbf{f}''_{i,x}(\hat{\mathbf{x}}_{k-1|k-1})\mathbf{P}_{k-1|k-1}(\mathbf{f}''_{j,x}(\hat{\mathbf{x}}_{k-1|k-1}))\mathbf{P}_{k-1|k-1})]_{ij}, \end{aligned} \tag{2.9}$$

where the state and covariance will be estimated. The Jacobian of $\mathbf{f}$ evaluated at the current estimate with respect to l is denoted $\mathbf{f}'_l(\hat{\mathbf{x}}_{k-1|k-1})$, $\mathbf{Q}$ is the covariance of the process noise and $\mathbf{f}''_{i,l}(\hat{\mathbf{x}}_{k-1|k-1})$ is the Hessian of row i with respect to l at the current estimate. $[a]_i$ means that the value a is present at position i in a vector, while $[b]_{ij}$ means that the value b is present at position i, j in a matrix.

The prediction step is followed by an update step. First, the Kalman gain ($\mathbf{K}_k$) is calculated as

$$\begin{aligned} \mathbf{S}_k &= \mathbf{R} + \mathbf{h}'_x(\hat{\mathbf{x}}_{k|k-1})\mathbf{P}_{k|k-1}(\mathbf{h}'_x(\hat{\mathbf{x}}_{k|k-1}))^T \\ &\quad + \frac{1}{2}[\mathrm{tr}(\mathbf{h}''_{i,x}(\hat{\mathbf{x}}_{k|k-1})\mathbf{P}_{k|k-1}(\mathbf{h}''_{j,x}(\hat{\mathbf{x}}_{k|k-1}))\mathbf{P}_{k|k-1})]_{ij} \\ \mathbf{K}_k &= \mathbf{P}_{k|k-1}(\mathbf{h}'_x(\hat{\mathbf{x}}_{k|k-1}))^T\mathbf{S}_k^{-1}, \end{aligned} \tag{2.10}$$

where $\mathbf{h}''_{i,l}(\hat{\mathbf{x}}_{k|k-1})$ is the Hessian of row i of $\mathbf{h}$ with respect to l. The Jacobian of $\mathbf{h}$ evaluated with respect to l at the current estimate is denoted $\mathbf{h}'_l(\hat{\mathbf{x}}_{k|k-1})$ and $\mathbf{R}$ is the covariance of the measurement noise, $\mathbf{v}$. The error between the prediction and the measurement is then calculated as

$$\epsilon_k = \mathbf{y}_k - \mathbf{h}\left(\hat{\mathbf{x}}_{k|k-1}\right) - \frac{1}{2}[\mathrm{tr}(\mathbf{h}''_{i,x}(\hat{\mathbf{x}}_{k|k-1})P_{k|k-1})]_i. \tag{2.11}$$

At the final step the states and the covariance is updated as

$$\begin{aligned} \hat{\mathbf{x}}_{k|k} &= \hat{\mathbf{x}}_{k|k-1} + \mathbf{K}_k \epsilon_k \\ \mathbf{P}_{k|k} &= \mathbf{P}_{k|k-1} - \mathbf{K}_k \mathbf{h}'_x(\hat{\mathbf{x}}_{k|k-1}) \mathbf{P}_{k|k-1} \end{aligned} \tag{2.12}$$

Notice that the first time the algorithm is run, initial values for the states, $\mathbf{x}$, and the covariance, $\mathbf{P}$, need to be supplied. For later runs the algorithm can be run iteratively. As noted in Gustafsson [2010] the prediction and update steps may switch place without affecting the estimation remarkably since the only difference will be in the first iteration. Another remark is that if the Hessians are set equal to zero in all the steps above, the first-order EKF is obtained.

2.3.2 Unscented Kalman filter (UKF)

The complexity, and in some extreme cases the impossibility, of calculating the Jacobians of a system is a significant drawback of the EKF [Julier and Uhlmann, 2004]. To avoid such calculations, a method that does not depend on Taylor series expansion must be used. By using the unscented transform it is possible to perform an approximate Kalman filtering without linearising the system. The unscented transform propagates sample points, called sigma-points, through the non-linearities to estimate mean and covariance.

Filtering using the above mentioned approach is called unscented Kalman filtering and there are numerous types of UKFs and they all have their advantages and disadvantages. One common classification is to divide the different types of UKFs into augmented and non-augmented algorithms, where the augmented UKF uses an augmented state vector for the process and measurement noise. Sun et al. [2009] state that the augmented UKF usually has improved accuracy but is more computationally demanding compared to the non-augmented UKF.

The UKF algorithm starts by defining weight matrices that depend on the design variables α, β and κ. Kandepu et al. [2008] suggest that α is set to a value between 0 and 1, that β should be equal to 2 if the noise is considered to be Gaussian distributed and Wu et al. [2005] states that κ is a scaling factor that is usually set to 0 or $3 - n$, where n is the number of states. However, κ needs to be a non-negative number to ensure the covariance matrix to be positive semi-definite. To make the equations easier to read, the constant λ has been used and it is defined as

$$\lambda = \alpha^2 (n + \kappa) - n \tag{2.13}$$

and the calculations of the weights are

$$
\begin{aligned}
W_m^0 &= \lambda / (n + \lambda) \\
W_c^0 &= \lambda / (n + \lambda) + 1 - \alpha^2 + \beta \\
W_m^i &= 1 / (2 (n + \lambda)), \quad i = 1, 2, \ldots, 2n \\
W_c^i &= 1 / (2 (n + \lambda)), \quad i = 1, 2, \ldots, 2n,
\end{aligned}
\tag{2.14}
$$

which are assembled into

$$
\begin{aligned}
\mathbf{W}_m &= \begin{bmatrix} W_m^0 & W_m^1 & \ldots & W_m^{2n} \end{bmatrix}^T \\
\mathbf{W}_c &= \begin{pmatrix} W_c^0 & 0 & \ldots & 0 \\ 0 & W_c^1 & \ddots & 0 \\ \vdots & \ddots & \ddots & \vdots \\ 0 & 0 & \ldots & W_c^{2n} \end{pmatrix}.
\end{aligned}
\tag{2.15}
$$

Like the EKF, the UKF consists of a prediction step and an update step. With a system as in (2.8) the non-augmented UKF can be outlined according to the following steps [Kandepu et al., 2008].

The prediction step starts by defining a sigma-point vector,

$$
\mathbf{X}_{k-1} = [\mathbf{m}_{k-1} \quad \ldots \quad \mathbf{m}_{k-1}] + \sqrt{n + \lambda} \begin{bmatrix} 0 & \sqrt{\mathbf{P}_{k-1}} & -\sqrt{\mathbf{P}_{k-1}} \end{bmatrix}, \tag{2.16}
$$

based on the prior mean, $\mathbf{m}_{k-1}$, and covariance, $\mathbf{P}_{k-1}$. This implies that the first time the algorithm is run, initial values of the mean and covariance must be supplied. The vector, $\mathbf{X}_{k-1}$, can be divided into single sigma points $\mathbf{X}_{k-1}^j$ for $j = 1, 2, \ldots, 2n + 1$. The points are then propagated through the non-linear function,

$$
\hat{\mathbf{X}}_k^j = \mathbf{f}\left(\mathbf{X}_{k-1}^j, u_{k-1}\right). \tag{2.17}
$$

By assembling all $\hat{\mathbf{X}}_k^j$ as

$$
\hat{\mathbf{X}}_k = \begin{bmatrix} \hat{\mathbf{X}}_k^1 & \ldots & \hat{\mathbf{X}}_k^{2n+1} \end{bmatrix} \tag{2.18}
$$

a new mean and covariance are predicted,

$$
\begin{aligned}
\bar{\mathbf{m}}_k &= \hat{\mathbf{X}}_k \mathbf{W}_m \\
\bar{\mathbf{P}}_k &= \hat{\mathbf{X}}_k \mathbf{W}_c \hat{\mathbf{X}}_k^T + \mathbf{Q}
\end{aligned}
\tag{2.19}
$$

where the covariance of the process noise is denoted $\mathbf{Q}$.

In the update step the sigma-points are redrawn,

$$\bar{\mathbf{X}}_k = [\bar{\mathbf{m}}_k \quad \ldots \quad \bar{\mathbf{m}}_k] + \sqrt{n+\lambda}\left[0 \quad \sqrt{\bar{\mathbf{P}}_k} \quad -\sqrt{\bar{\mathbf{P}}_k}\right]. \tag{2.20}$$

They are then propagated through the measurement function,

$$\bar{\mathbf{Y}}_k^j = \mathbf{h}\left(\bar{\mathbf{X}}_k^j\right) \tag{2.21}$$

and eventually a Kalman filter gain is calculated,

$$\begin{aligned} \mathbf{S}_k &= \bar{\mathbf{Y}}_k \mathbf{W}_c \bar{\mathbf{Y}}_k^T + \mathbf{R} \\ \mathbf{C}_k &= \bar{\mathbf{X}}_k \mathbf{W}_c \bar{\mathbf{Y}}_k^T \\ \mathbf{K}_k &= \mathbf{C}_k \mathbf{S}_k^{-1}. \end{aligned} \tag{2.22}$$

The matrix $\mathbf{R}$ is the covariance matrix for the measurement noise. At last, the estimated mean and covariance are updated

$$\begin{aligned} \bar{\mu}_k &= \bar{\mathbf{Y}}_k \mathbf{W}_m \\ \mathbf{m}_k &= \bar{\mathbf{m}}_k + \mathbf{K}_k\left(\mathbf{y}_k - \bar{\mu}_k\right) \\ \mathbf{P}_k &= \bar{\mathbf{P}}_k - \mathbf{K}_k \mathbf{S}_k \mathbf{K}_k^T. \end{aligned} \tag{2.23}$$

As in Sun et al. [2009], the UKF is often claimed to be more accurate than the first-order EKF and while its accuracy often is close to the one of the second-order EKF, this is not always true. In Gustafsson [2010] it is shown that the UKF may perform worse than the EKF in some cases. This comes from the fact that the sigma-points risk being poorly chosen and may be unable to capture the characteristics of the non-linearities properly. So the choice of non-linear filter should depend on the non-linearities of the application and hence on the application itself.

Part II

Modelling and Controller Design

3

Modelling

This chapter describes how the modelling of the loudspeaker was done and explains the approximations that have been used. Initially, the loudspeaker model will be presented as an electrical circuit. This circuit will be used to derive a complete state-space model. Finally, the model that has been used for the amplifier unit during the experiments is presented.

3.1 The loudspeaker model

An easy and common way to model a loudspeaker is to use an electrical equivalent circuit. One of the most common is the Thiele-Small model. The name comes from the creators, A. N. Thiele who laid the ground to it and R. H. Small who continued on Thiele's model and developed it further. The work of Thiele was first published the year 1971 in two parts, Thiele [1971a] and Thiele [1971b], while Small's work was published in Small [1972].

The circuit in Small [1972] models the performance of the moving-coil loudspeaker for low frequencies with small amplitudes. This is also called the small signal domain. In practice, this is when the cone displacement of the speaker is very small. Because of the small displacement it is plausible to assume that the speaker is linear like the model but for bigger cone excursions this is not true and a non-linear model is needed. The notion of a loudspeaker as a non-linear system was accepted quite recently and the fact that numerous parameters depend on several other parameters makes a loudspeaker difficult to model, and approximations become necessary.

To include the non-linearities in the model, some changes have to be made to the original one. The model that Jakobsson and Larsson [2010] used was the LR-2 model, which is shown in Figure 3.1. This model is an extension of the Thiele-Small model that describes the eddy currents, that occur at higher frequencies, more accurately.

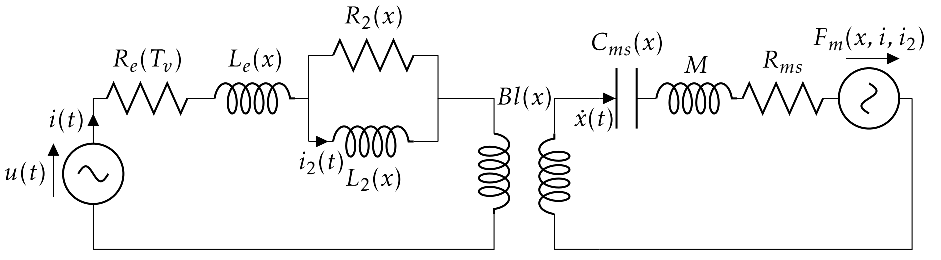

Figure 3.1: *Equivalent circuit of a moving-coil loudspeaker.*

From the left side of the circuit in Figure 3.1 it is possible to derive expressions of the terminal voltage, $u(t)$, and the voltage drop over R_2 and L_2 using Kirchhoff's current and voltage laws. This results in

$$u(t) = i(t)R_e(T_v) + \frac{d\Big(L_e(x)i(t)\Big)}{dt} + \frac{d\Big(L_2(x)i_2(t)\Big)}{dt} + Bl(x)\frac{dx(t)}{dt}, \tag{3.1}$$

where x is the cone displacement and T_v is the temperature of the voice coil, and

$$\frac{d\Big(L_2(x)i_2(t)\Big)}{dt} = \Big(i(t) - i_2(t)\Big)R_2(x). \tag{3.2}$$

Since the right side of the circuit corresponds to the mechanical part of the system it is possible to use Newton's second law and get

$$Bl(x)i(t) - F_m(x,i,i_2) = M\frac{d^2x(t)}{dt^2} + R_{ms}\frac{dx(t)}{dt} + \frac{x}{C_{ms}(x)} \tag{3.3}$$

where $Bl(x) - F_m(x,i,i_2)$ is the resulting force on the voice-coil. Bai and Huang [2009] developed an approximation of $F_m(x,i,i_2)$ according to

$$F_m(x,i,i_2) \approx -\frac{i^2(t)}{2}\frac{dL_e(x)}{dx} - \frac{i_2^2(t)}{2}\frac{dL_2(x)}{dx}. \tag{3.4}$$

In control theory, equations are often written in state-space form and if (3.1) - (3.4) above are manipulated it is possible to acquire

$$\frac{d^2x(t)}{dt^2} = \frac{1}{M}\Big(- \frac{x(t)}{C_{ms}(x)} - R_{ms}\frac{dx(t)}{dt} + i(t)\Big(Bl(x) + \frac{1}{2}\frac{dL_e(x)}{dx}i(t)\Big) + \frac{1}{2}\frac{dL_2(x)}{dx}i_2^2(t)\Big), \tag{3.5}$$

$$\frac{di(t)}{dt} = \frac{1}{L_e(x)}\Big(- \frac{dx}{dt}\Big(Bl(x) + \frac{dL_e(x)}{dx}i(t)\Big) - i(t)\Big(R_e(T_v) + R_2(x)\Big) + i_2(t)R_2(x) + u(t)\Big) \tag{3.6}$$

and

$$\frac{di_2(t)}{dt} = \frac{1}{L_2(x)}\Big(i(t)R_2(x) - i_2(t)\Big(R_2(x) + \frac{dL_2(x)}{dx}\frac{dx}{dt}\Big)\Big). \tag{3.7}$$

The complete state-space vector can be chosen as

$$\mathbf{x} = [x(t)\ \ \dot{x}(t)\ \ i(t)\ \ i_2(t)]^{\mathrm{T}} = [x_1\ \ x_2\ \ x_3\ \ x_4]^{\mathrm{T}}. \tag{3.8}$$

With (3.5) to (3.8) the equation for the dynamics can be written as

$$\dot{\mathbf{x}} = f(\mathbf{x}) + g(\mathbf{x})u. \tag{3.9}$$

A more convenient way to bundle the equations is to write them using matrices. Note that, because the equations are non-linear some states are also present inside the matrices. The state-space description can be written as

$$\dot{\mathbf{x}} = \begin{bmatrix} 0 & 1 & 0 & 0 \\ \frac{-1}{MC_{ms}(x_1)} & \frac{-R_{ms}}{M} & \frac{Bl(x_1)+\frac{1}{2}\frac{dL_e(x_1)}{dx_1}x_3}{M} & \frac{\frac{1}{2}\frac{dL_2(x_1)}{dx_1}x_4}{M} \\ 0 & \frac{-Bl(x_1)-\frac{dL_e(x_1)}{dx_1}x_3}{L_e(x_1)} & \frac{-R_e(T_v)-R_2(x_1)}{L_e(x_1)} & \frac{R_2(x_1)}{L_e(x_1)} \\ 0 & 0 & \frac{R_2(x_1)}{L_2(x_1)} & \frac{-R_2(x_1)-\frac{dL_2(x_1)}{dx_1}x_2}{L_2(x_1)} \end{bmatrix}\mathbf{x} + \begin{bmatrix} 0 \\ 0 \\ \frac{1}{L_e(x_1)} \\ 0 \end{bmatrix}u. \tag{3.10}$$

3.2 Non-linearities

It is extremely hard to make an exact model of a loudspeaker because of all the non-linearities that must be taken into account. Due to the complexity of modelling the non-linearities some approximations have been made in this thesis.

One dependency that is missing in the model is the fact that many loudspeaker parameters are influenced by the temperature. In Øyen [2007], the parameters that are known to be affected by the voice-coil temperature when working in the large signal domain are considered to be $R_e, Bl(x), C_{ms}(x)$ and $L_e(x)$. The impedances represented by $R_2(x)$ and $L_2(x)$ are also non-linear and have the same behaviour as $L_e(x)$ but only influence when the system gets signals with high frequencies according to Klippel [2003]. Since the signals that will be used in this thesis have relatively low frequencies, these functions will be regarded as constants.

The functions $Bl(x), C_{ms}(x)$ and $L_e(x)$ have similar appearances for all speakers but their amplitudes can be significantly different from one model to another. To get an idea what the non-linearities look like, Jakobsson and Larsson [2010] sent a speaker to Klippel's measurement service. The service is supplied by Klippel GmbH who conducts experiments to measure the loudspeaker parameters. Klippel's service returned coefficients for a polynomial fit for each non-linearity that were valid in a specified range. Due to this polynomial it was possible for the functions to render negative values outside the fitted range. Since negative impedances are impossible to realise in practice, Jakobsson and Larsson [2010] came up with solutions to generate a more realistic fit for each function.

3.2.1 Force factor $Bl(x)$

Since the force factor has its maximum value when the displacement is close to zero, as described in Section 2.1.1 on page 8, the values of the function could be negative if the displacement went outside the fitted range when using the polynomial supplied by Klippel. Jakobsson and Larsson [2010] used a Gaussian sum, which was fitted to the polynomial, to avoid this. The resulting function can be seen in Figure 3.2 on the facing page and can be expressed as

$$Bl(x) = \sum_{n}^{N} \alpha_n e^{-\frac{(x-x_n)^2}{2\sigma^2}} \tag{3.11}$$

where a_n, x_n and σ are constants. The derivative can be described as

$$\frac{dBl(x)}{dx} = \sum_{n}^{N} \alpha_n \frac{x_n - x}{\sigma^2} e^{-\frac{(x-x_n)^2}{2\sigma^2}}. \tag{3.12}$$

3.2.2 Suspension compliance $C_{ms}(x)$

As mentioned in Section 2.1.2 on page 8, the suspension compliance tries to fixate the voice-coil at the resting position. By using Fourier transform, the impedance of the suspension compliance can be written as

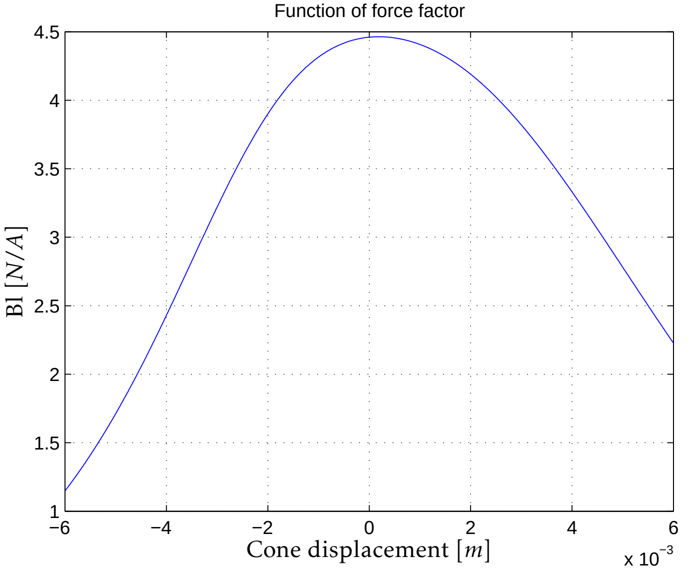

Figure 3.2: *The non-linear function of the force factor represented as a Gaussian sum.*

$$Z_{C_{ms}}(\omega) = \frac{1}{i\omega C_{ms}(x)}. \tag{3.13}$$

The suspension's impedance will increase when the cone leaves its equilibrium and hence $C_{ms}(x)$ must be reduced outside the equilibrium. This means that the suspension compliance shares the same characteristics as the force factor. Since they have the same behaviour they will be modelled and fitted with the same equations, (3.11) and derivative (3.12), but with different numerical values. A suspension compliance function using Gaussian sums fitted to the polynomial supplied by Klippel, can be seen in Figure 3.3 on the following page.

3.2.3 Voice-coil inductance $L_e(x)$

The voice-coil inductance also has a displacement dependency but does not share characteristics with the force factor and the suspension compliance. The value of the inductance gets higher when the voice-coil moves inwards and decreases when it is moving outwards. This is due to the magnetic field created by the current passing through the voice-coil. Jakobsson and Larsson [2010] captured this behaviour by using a sigmoid function, as in Figure 3.4 on page 25. The sigmoid function is defined as

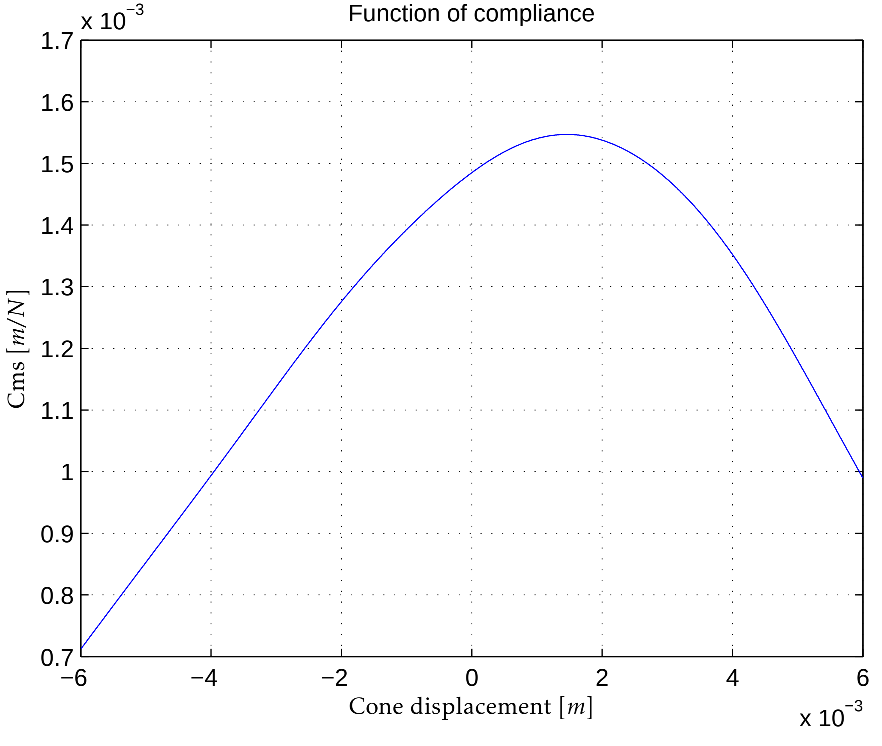

Figure 3.3: *The non-linear function of the suspension compliance represented as a Gaussian sum.*

$$L_e(x) = \frac{L_1}{1 + e^{-a(x-x_0)}} + L_0 \tag{3.14}$$

where L_0, L_1 and x_0 are constants. The first-order derivative of this function is

$$\frac{dL_e(x)}{dx} = \frac{aL_1 e^{-a(x-x_0)}}{(1 + e^{-a(x-x_0)})^2} \tag{3.15}$$

while the second-order derivative can be written as

$$\frac{d^2L_e(x)}{dx^2} = \frac{a^2L_1 e^{-a(x-x_0)}}{(1 + e^{-a(x-x_0)})^2}\Big(\frac{2e^{-a(x-x_0)}}{1 + e^{-a(x-x_0)}} - 1\Big). \tag{3.16}$$

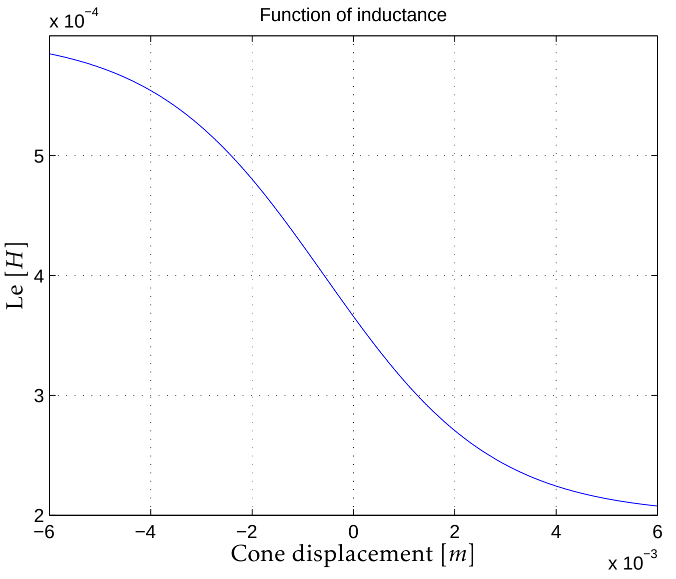

Figure 3.4: *The non-linear function of the voice-coil inductance represented as a sigmoid function.*

3.2.4 Impedance

A way to determine a loudspeaker's characteristics is to measure the impedance. It is possible to analyse the speaker based on how it behaves at different frequencies. An example of how the impedance can change with frequency can be seen in Figure 3.5 on the following page. The peak in the middle of the figure is the speaker's resonance frequency.

By knowing the impedance it is possible to get a set of parameters for the model. This is done by using a chirp signal that starts as a low frequency sine wave and raises the frequency with time until it reaches a desired end frequency. To create a function of the impedance, the most common and easy way is to use Ohm's law. In the Laplacian domain the law can be written as

$$U(s) = Z(s) \cdot I(s). \tag{3.17}$$

An approximate function of the speaker's impedance can be acquired by linearisation around the equilibrium. The approximation is valid for small signals that generate small cone excursions. By using that, it is possible to match a measured impedance curve to it to receive proper parameter values. In Seidel and Klippel [2001] the impedance of the used loudspeaker model is derived and the result is

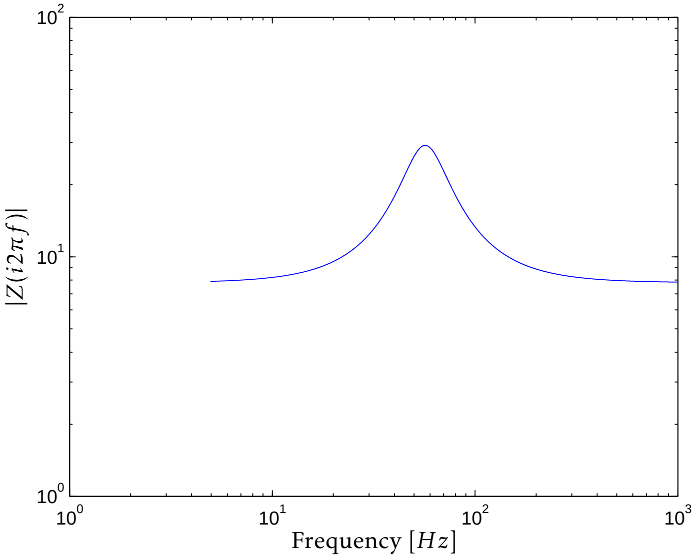

Figure 3.5: *Amplitude of a loudspeaker's impedance in the frequency domain.*

$$Z(s) = \frac{sL_{ces}}{s^2 L_{ces} C_{mes} + \frac{sL_{ces}}{R_{es}} + 1} + \frac{sL_2 R_2}{sL_2 + R_2} + sL_e + R_e \tag{3.18}$$

where

$$L_{ces} = C_{ms}(Bl)^2, \qquad C_{mes} = \frac{M_{ms}}{(Bl)^2}, \qquad R_{es} = \frac{(Bl)^2}{R_{ms}}. \tag{3.19}$$

C_{ms}, L_e and Bl are the suspension compliance, voice-coil inductance and force factor evaluated at the cone's resting position.

3.3 The amplifier model

The amplifier that has been used in experiments was unable to amplify DC signals. To include that fact, the amplifier was modelled as a high-pass filter according to

$$\begin{aligned} \tau \dot{u}_{amp} &= u - u_{amp} \\ e &= V_{amp}(u - u_{amp}) \end{aligned} \tag{3.20}$$

where u_{amp} is the voltage distortion, τ is a time constant, V_{amp} is an amplification constant, u is the control signal from the controller and e is the output sent to the loudspeaker [Fränken et al., 2005]. The state-space model can be written using a transfer function from input voltage, u, to output voltage, e, as

$$E(s) = V_{amp} \cdot \frac{s\tau}{1 + s\tau} U(s). \tag{3.21}$$

By taking this model into account, when calculating the control signal, it is possible to reduce the need for a proper DC amplifier.

4

Controller

This chapter contains details about how the different controllers and state estimators have been designed. The main controller is based on exact input-output linearisation and uses state estimators with feed-forward or observer-based design. Additionally, a simple PID controller of the terminal current has been designed for comparison and a controller that uses both PID and feed-forward from reference. For all methods that use feedback, the measurement, y, has consisted of the terminal current, i. The controllers in this chapter are designed for amplifiers that can handle DC components and hence the amplifier model from Section 3.3 will not be used. The modifications that had to be made to the controllers due to the AC amplifier are described in Chapter 6.

4.1 Exact input-output linearisation

To be able to apply a linear control strategy, the non-linear system needs to be linearised. As explained in Chapter 2, a simple approach is to approximate the non-linearities using partial derivatives evaluated at an equilibrium. This will generate an approximate model that is only valid close to the equilibrium and that may be inaccurate as soon as the system leaves that state. Instead, the exact input-output linearisation method described in Chapter 2 has been used to linearise the system exactly. Exact input-output linearisation will render a system according to Figure 4.1 on the next page, and can be divided into two parts, inverse dynamics (ID) and linear dynamics (LD).

The inverse dynamics is described by a control law to form a new input for the system that cancels both the linear and the non-linear dynamics. In order to acquire this control law, the time derivative of the output must be used, but in

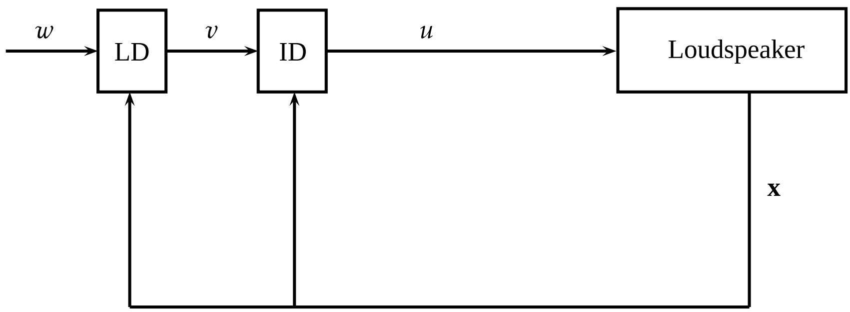

Figure 4.1: *Diagram of the system with a controller based on exact input-output linearisation.*

the loudspeaker model there is no output specified. Glad and Ljung [2009] recommend the possibility to chose a suitable output for further calculations. The position, x, has been chosen as the output to receive relatively simple expressions for its derivatives. By following the steps in Chapter 2 and using the control law in (2.6), the input to the loudspeaker will be

$$
\begin{aligned}
u = \Bigg\{ & Mv + \frac{x_2}{C_{ms}(x_1)}\left(1 - \frac{x_1}{C_{ms}(x_1)} \cdot \frac{dC_{ms}(x_1)}{dx_1}\right) \\
& + \frac{R_{ms}}{M}\left(\frac{-x_1}{C_{ms}(x_1)} - R_{ms}x_2 + \left(Bl(x_1) + \frac{1}{2} \cdot \frac{dL_e(x_1)}{dx_1}x_3\right)x_3 + \frac{1}{2} \cdot \frac{dL_2(x_1)}{dx_1}x_4^2\right) \\
& - x_2x_3\frac{dBl(x_1)}{dx_1} - \frac{1}{2}x_2x_3^2\frac{d^2L_e(x_1)}{dx_1{}^2} - \frac{1}{2}x_2x_4^2\frac{d^2L_2(x_1)}{dx_1{}^2} \\
& - \frac{x_4}{L_2(x_1)} \cdot \frac{dL_2(x_1)}{dx_1}\left(R_2(x_1)x_3 - \left(R_2(x_1) - x_2\frac{dL_2(x_1)}{dx_1}\right)x_4\right)\Bigg\} \\
& \cdot \left(\frac{L_e(x_1)}{Bl(x_1) + x_3\frac{dL_e(x_1)}{dx_1}}\right) + Bl(x_1)x_2 + x_2x_3\frac{dL_e(x_1)}{dx_1} + R_ex_3 + R_2x_3 - R_2x_4
\end{aligned}
\tag{4.1}
$$

where $x_1, ..., x_4$ are the system's states [Jakobsson and Larsson, 2010].

While deriving the control law for u, the relative degree of the system was found to be equal to three. Since there are four states this means that there will be, possibly harmful, zero dynamics present in the system. How the zero dynamics will affect the system depends on the transformation from the state vector $\mathbf{x}$ to the new state vector $\mathbf{z}$. With position x as the choice of output, the transformation becomes

$$\mathbf{z} = [x_1 \;\; x_2 \;\; \dot{x}_2 \;\; \Psi]^T \tag{4.2}$$

where Ψ may be chosen arbitrarily as long as

$$L_g \Psi = 0 \tag{4.3}$$

holds.

In Jakobsson and Larsson [2010], z_4 was chosen equal to i_2 and it was shown that this choice rendered stable, and hence harmless, zero dynamics. By using z_4 equal to i_2 the new state vector $\mathbf{z}$ can be expressed as

$$\begin{aligned}
z_1 &= x_1 \\
z_2 &= x_2 \\
z_3 &= \frac{1}{M}\left(\frac{-x_1}{C_{ms}(x_1)} - R_{ms}x_2 + Bl(x_1)x_3 + \frac{1}{2}\cdot\frac{dL_e(x_1)}{dx_1}x_3^2 + \frac{1}{2}\cdot\frac{dL_2(x_1)}{dx_1}x_4^2\right) \\
z_4 &= x_4
\end{aligned} \tag{4.4}$$

and this will be important when designing the linear dynamics of the system. The linear dynamics are based upon the ideas of pole placement for full state feedback, which is described in Glad and Ljung [2008]. The control law for v can be expressed as

$$v = -k_1 z_1 - k_2 z_2 - k_3 z_3 - k_4 z_4 + k_{amp} w \tag{4.5}$$

where v is the input to the ID block in Figure 4.1 on the facing page. The values $k_1, ..., k_4$ in (4.5) are constants based on the pole placement and k_{amp} is some amplification to the input to receive a proper amplitude of the output. The value of k_{amp} can therefore be chosen freely but if it is chosen too large an implementation may lead to severe saturations, while a too small k_{amp} may lead to insufficient amplitude of the control signal. To determine $k_1, ..., k_4$ an investigation of the system's poles could be utilised.

The transformed state-space description

$$\dot{\mathbf{z}} = \begin{bmatrix} 0 & 1 & 0 & 0 \\ 0 & 0 & 1 & 0 \\ -k_1 & -k_2 & -k_3 & -k_4 \\ p_1 & p_2 & p_3 & -\frac{R_2}{L_2} \end{bmatrix} \mathbf{z} + \begin{bmatrix} 0 \\ 0 \\ k_{amp} \\ 0 \end{bmatrix} w \tag{4.6}$$

can be derived from (4.4). The constants $k_1, ..., k_4$ are identical to the ones in (4.5) while $p_1, ..., p_3$ are some possibly non-linear expressions. The term $-\frac{R_2}{L_2}$ comes from the fact that $\dot{z}_4 = \dot{x}_4$, and that L_2 are considered constant.

By choosing k_4 equal to 0 it is possible to acquire a linear system with a well-defined characteristic equation. This makes the characteristic equation equal to

$$s^4 + \left(k_3 + \frac{R_2}{L_2}\right)s^3 + \left(k_2 + \frac{R_2}{L_2}k_3\right)s^2 + \left(k_1 + \frac{R_2}{L_2}k_2\right)s + \frac{R_2}{L_2}k_1 = 0. \tag{4.7}$$

Now the characteristic equation in (4.7) needs to be mapped to the characteristic equation of the desired poles. A straightforward way to choose the desired poles, in line with Jakobsson and Larsson [2010], is to use the poles of the loudspeaker model when linearised around the equilibrium. In that way the controlled loudspeaker will behave approximately like an uncontrolled loudspeaker for small inputs. After linearising the loudspeaker around $x = 0$, the system can be written on the form $\dot{\mathbf{x}} = A\mathbf{x} + Bu$ where the A matrix is equal to

$$A = \begin{bmatrix} 0 & 1 & 0 & 0 \\ -\frac{1}{MC_{ms}} & -\frac{R_{ms}}{M} & \frac{Bl}{M} & 0 \\ 0 & -\frac{Bl}{L_e} & -\frac{R_e+R_2}{L_e} & \frac{R_2}{L_e} \\ 0 & 0 & \frac{R_2}{L_2} & -\frac{R_2}{L_2} \end{bmatrix}. \tag{4.8}$$

The characteristic equation of the system given by (4.8) is

$$\begin{aligned} &s^4 + \left(\frac{R_2}{L_2} + \frac{R_e}{L_e} + \frac{R_2}{L_e} + \frac{R_{ms}}{M}\right)s^3 \\ &+ \left(\frac{R_eR_2}{L_eL_2} + \frac{R_{ms}R_2}{ML_2} + \frac{R_{ms}R_e}{ML_e} + \frac{R_{ms}R_2}{ML_e} + \frac{(Bl)^2}{ML_e} + \frac{1}{MC_{ms}}\right)s^2 \\ &+ \left(\frac{R_{ms}R_eR_2}{ML_eL_2} + \frac{(Bl)^2\,R_2}{ML_eL_2} + \frac{R_2}{MC_{ms}L_2} + \frac{R_e}{MC_{ms}L_e} + \frac{R_2}{MC_{ms}L_e}\right)s + \frac{R_eR_2}{MC_{ms}L_eL_2} = 0. \end{aligned} \tag{4.9}$$

This results in an overdetermined set of equations where $k_1, ..., k_3$ was chosen by applying a least-squares algorithm to set the coefficients in (4.7) as close to the ones in (4.9) as possible. As mentioned in Jakobsson and Larsson [2010], the linearised system may not be exactly the system that is wanted. The poles may need to be scaled with a common constant to achieve proper speed of the system. If they are too slow the system may not compensate fast enough, while if the poles are too fast there is a risk that they require a sample rate that is faster than the hardware can handle.

4.2 State estimation

For the controller based on exact linearisation it is vital to receive information about all states at all times. To be able to provide such information, several state estimators have been designed.

4.2.1 Feed-forward state estimation

The feed-forward state estimator is the most simple estimator designed in this thesis. By using a model of the loudspeaker it is possible to estimate the states of the real system and feed the controller with them. A diagram of the set-up can be seen in Figure 4.2. This approach of using a state-space model together with some exact input-output linearisation has been proven to efficiently invert non-linear systems in various cases [Hirschorn, 1979].

Because of the fact that this method uses no feedback from the real system it is relatively easy to implement and does not need any measuring devices, which will render a smaller cost. One major drawback is that without feedback the estimation will be highly sensitive to model errors, such as inaccurate parameter values, and has no means to correct itself online.

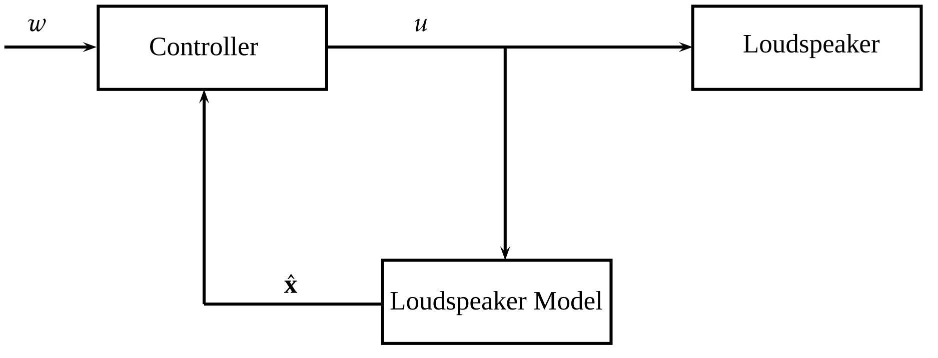

Figure 4.2: *Diagram of the system when using feed-forward state estimation.*

4.2.2 Observer-based state estimation

Another way of estimating the states is to use an observer. In Figure 4.3 there is a diagram of the entire system when using an observer-based state estimator. Observers are more complex than the feed forward approach and need some feedback from the true system. A common way to design an observer is to involve some kind of filtering. In Chapter 2, the ideas of non-linear filtering for estimation using the extended Kalman filter (EKF) and the unscented Kalman filter (UKF) are outlined and based on these techniques, several observers have been designed.

As mentioned earlier in Chapter 2, the EKF requires Jacobians of the system to be calculated. The Jacobians that have been used when designing the EKF are

$$\mathbf{h}'_x = [0 \;\; 0 \;\; 1 \;\; 0]^T \tag{4.10}$$

and

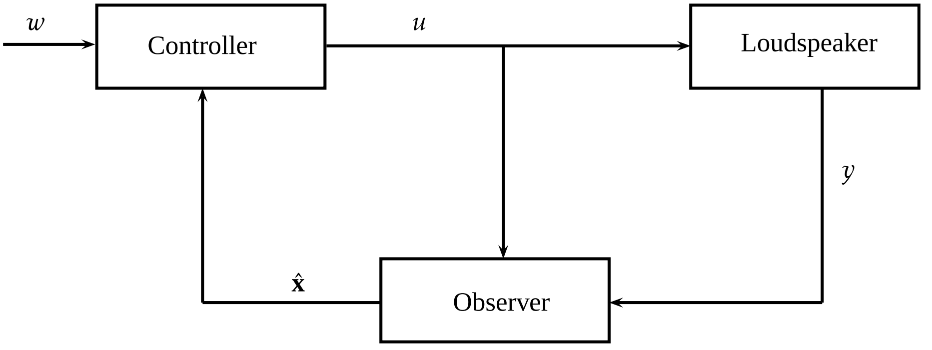

Figure 4.3: *Diagram of the system when using observer-based state estimation.*

$$\mathbf{f}'_x = \begin{pmatrix} 0 & 1 & 0 & 0 \\ f_{2,1} & -\frac{R_{ms}}{M} & \frac{Bl(x_1)}{M} + \frac{dL_e(x_1)}{dx_1} \cdot \frac{x_3}{M} & 0 \\ f_{3,1} & -\frac{Bl(x_1)+\frac{dL_e(x_1)}{dx_1}x_3}{L_e(x_1)} & -\frac{\frac{dL_e(x_1)}{dx_1}x_2+R_e+R_2}{L_e(x_1)} & \frac{R_2}{L_e(x_1)} \\ 0 & 0 & \frac{R_2}{L_2} & -\frac{R_2}{L_2} \end{pmatrix} \tag{4.11}$$

when considering R_2 and L_2 as constants.

Some expressions in (4.11) are marked $f_{i,j}$ to make the matrix easily perspicuous. These terms can be explicitly written as

$$f_{2,1} = x_1 \frac{\frac{dC_{ms}(x_1)}{dx_1}}{MC_{ms}(x_1)^2} - \frac{1}{MC_{ms}(x_1)} + \frac{dBl(x_1)}{dx_1} \cdot \frac{x_3}{M} + \frac{x_3^2}{2M} \cdot \frac{d^2L_e(x_1)}{dx_1^2} \tag{4.12}$$

and

$$\begin{aligned} f_{3,1} = & -\frac{\frac{dBl(x_1)}{dx_1}x_2 + \frac{d^2L_e(x_1)}{dx_1^2}x_2x_3}{L_e(x_1)} + \frac{\left(Bl(x_1)x_2 + x_2x_3\frac{dL_e(x_1)}{dx_1}\right)\frac{dL_e(x_1)}{dx_1}}{L_e(x_1)^2} \\ & + \frac{(R_e + R_2x_1)x_3\frac{dL_e(x_1)}{dx_1}}{L_e(x_1)^2} - \frac{R_2x_1x_4\frac{dL_e(x_1)}{dx_1}}{L_e(x_1)^2}. \end{aligned} \tag{4.13}$$

When using the second-order EKF, Hessians are needed as well. In this case they become very complex matrices and will therefore not be written explicitly. Each differential equation, f_j, in the model will render a Hessian according to

$$
\mathbf{f}''_{f_j,x} = \begin{bmatrix}
\frac{\partial^2 f_j}{\partial x_1^2} & \frac{\partial^2 f_j}{\partial x_1\,\partial x_2} & \frac{\partial^2 f_j}{\partial x_1\,\partial x_3} & \frac{\partial^2 f_j}{\partial x_1\,\partial x_4} \\
\frac{\partial^2 f_j}{\partial x_2\,\partial x_1} & \frac{\partial^2 f_j}{\partial x_2^2} & \frac{\partial^2 f_j}{\partial x_2\,\partial x_3} & \frac{\partial^2 f_j}{\partial x_2\,\partial x_4} \\
\frac{\partial^2 f_j}{\partial x_3\,\partial x_1} & \frac{\partial^2 f_j}{\partial x_3\,\partial x_2} & \frac{\partial^2 f_j}{\partial x_3^2} & \frac{\partial^2 f_j}{\partial x_3\,\partial x_4} \\
\frac{\partial^2 f_j}{\partial x_4\,\partial x_1} & \frac{\partial^2 f_j}{\partial x_4\,\partial x_2} & \frac{\partial^2 f_j}{\partial x_4\,\partial x_3} & \frac{\partial^2 f_j}{\partial x_4^2}
\end{bmatrix}. \tag{4.14}
$$

One major issue when designing an observer is that the noise covariances, **Q** and **R**, and especially the relationship between them need to be well tuned for the estimation to function properly. In Glad and Ljung [2009] there are some tips for tuning these matrices which have been used to find satisfying values. The matrices have initially been assumed to be diagonal and non-diagonal elements have only been used when necessary. When the assumed process noise is smaller than the true process noise the state estimation may not be fast enough to follow the true states. So by assuming low process noise and raise it until the estimations are satisfying it is possible to find a good value for Q. When tuning R it is possible to start by assuming low measurement noise and raise it until the estimations are smooth enough. This is because of the fact that if the measurement noise is assumed too small, the true measurement noise will make the estimations very noisy.

In addition to the original UKF designed in Jakobsson and Larsson [2010], an augmented UKF has been designed. When it comes to estimation, as stated in Chapter 2, an augmented UKF is often superior to a non-augmented one. Another advantage with the augmented UKF is that it is relatively straightforward to introduce non-additive process noise which could be used to express inaccuracy in parameter values or similar. The augmented state vector is

$$
\mathbf{x}_a = \begin{bmatrix} \mathbf{x}^T & \mathbf{W}^T & \mathbf{V}^T \end{bmatrix}^T, \tag{4.15}
$$

where $\mathbf{x}$ is the original state vector, $\mathbf{W}$ is a vector that contains the process noise variables and $\mathbf{V}$ is a vector that contains the measurement noise variables.

The steps of the augmented UKF algorithm are almost the same as for the non-augmented UKF algorithm. The only difference is that the sigma-points do not need to be redrawn in the update step because of the augmented state vector.

4.3 PID controller

One state that only requires simple tools to measure and has a low cost to measure is x_3 (the terminal current i). A common controller is a proportional-integral-derivative controller (PID controller) which is used in many applications worldwide [Glad and Ljung, 2008]. The PID controller can be written as

$$u(t) = K \cdot (e(t) + \frac{1}{T_i} \int_0^t e(\tau)\,\mathrm{d}\tau + T_d \frac{de(t)}{dt}) \tag{4.16}$$

where $e(t)$ is the control error and K, T_i and T_d are design parameters. To avoid the pure derivative in implementations, it is often approximated by a low-pass filtered version. A low-pass filtered derivative can be written as

$$T_d s \approx \frac{T_d s}{\mu T_d s + 1} \tag{4.17}$$

in Laplacian domain, where μ is another design parameter which can be tuned to set a proper cut-off frequency.

The input to the loudspeaker needs to be a specified voltage and since the current is measured it needs to be transformed into voltage. An easy and common way to convert the current into voltage is to use Ohm's law, (3.17). It states that the current times the impedance is equal to the voltage. The impedance for the model, Figure 3.1 on page 20, can be seen in (3.18), and is derived in Seidel and Klippel [2001]. By using this, the implementation is straightforward with a controller adjusting the current and then transforming it into a suitable voltage input to the loudspeaker.

4.4 Feed-forward from reference with feedback

When it is possible to measure a state, it is almost always useful to use this information for control. The main idea with using a feed-forward controller together with feedback is to estimate the states using the feed-forward controller and additionally use the information from the measurements to handle model errors.

This is achieved by calculating the difference between the output from the model and the real system as can be seen in Figure 4.4 on the next page. If the difference is zero, the model has generated the correct output and no compensation is needed to the input to the loudspeaker. If the difference is non-zero, the PID controller will try to adjust the difference by adding its control signal to the input of the loudspeaker.

When measuring the current, i, the output of the PID controller needs to be con-

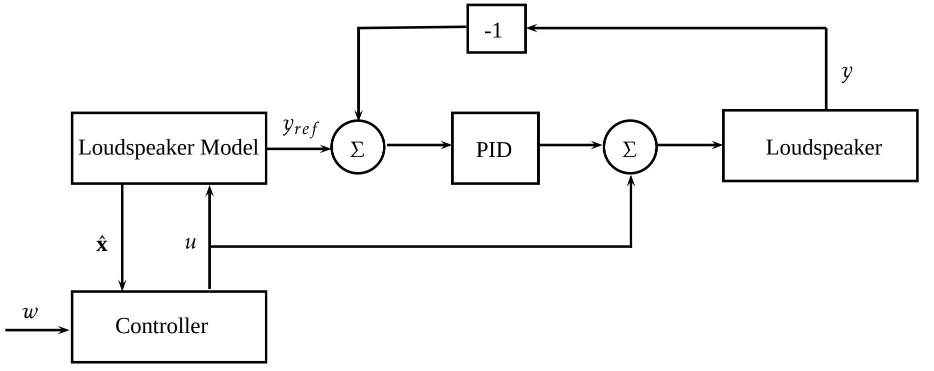

Figure 4.4: *Diagram of the system when using feed-forward from reference with feedback.*

verted to voltage. By using the impedance $Z(s)$, the converted signal $u_{PID}(t)$ can be written in Laplacian domain as

$$U_{PID}(s) = Z(s)I_{PID}(s) \tag{4.18}$$

where $I_{PID}(s)$ is the Laplace transform of the output from the PID controller.

Part III

Results

5 Simulations

During this thesis, multiple methods have been verified via simulations and some of them have been implemented and evaluated via physical experiments. The simulated loudspeaker used the same parameter values as Jakobsson and Larsson [2010], while the physical experiments were conducted on similar but not identical loudspeakers. This chapter displays the results from simulations of the different approaches. The simulations have been performed with an emphasis on comparing different controller and noise settings and less focus on model validation, which has been investigated by Jakobsson and Larsson [2010]. They showed that the used model works as a good approximation, at least for the non-linearities, of the system.

When measuring the level of distortion, the total harmonic distortion (THD) measure has been used. The definition of THD is

$$\mathrm{THD} = \frac{\sqrt{\sum_{i=2}^{\infty} |P_i|^2}}{|P_1|} \tag{5.1}$$

where P_i is the amplitude of the i:th harmonic and P_1 is the amplitude of the fundamental tone. It is however impossible to use an infinite number of harmonics and based on the fact that their amplitude is decreasing with higher numbers, only the first six harmonics were used. Another risk when handling too many harmonics is that aliasing effects might occur if the sample rate is too low.

When it comes to analysing the results, THD is difficult to compare in terms of audibility. This issue is further addressed in Chapter 7.

5.1 Simulation set-up

To test the different control strategies, initial simulations were performed to get an understanding if there would be any possible success in implementing them on a real system. All simulations were done using Simulink, which is a package in Matlab. Simulink is made for modelling, simulating and analysing dynamic systems.

Jakobsson and Larsson [2010] showed that the non-compensated and the compensated system behave similarly when fed with various levels of input voltage. The difference was that the results were scaled with the voltage. The single parameter from Jakobsson and Larsson [2010] that affected the controllers the most was the frequency of the input signal.

The new simulations were performed with a sinusoidal input signal with an amplitude of five volts, but varying frequency. To capture the fact that it is almost impossible to get the loudspeaker's parameters completely accurate, a random value was added to the parameters in all simulations, except when the standard deviation was equal to zero, then the original values were kept. This can be expressed as

$$\begin{aligned} P_{val} &:= P_{val} \cdot (1 + \mathbb{X}) \\ \mathbb{X} &\sim \mathcal{N}(0, \sigma) \end{aligned} \tag{5.2}$$

where P_{val} is the parameter value and $\mathcal{N}(0, \sigma)$ means that the variable is Gaussian distributed with mean equal to zero and standard deviation equal to σ. Because of the fact that a new value was generated every run, each frequency was simulated 100 times to make the results more statistically reliable. The resulting THD was then calculated as the mean of the THD for each run. Notice that all parameter perturbations for the loudspeaker were pre-calculated and could therefore be reused when simulating the different approaches. This prevents unreliable results that may occur when generating new values for each controller method.

The simulation time was set equal to two seconds after studying the loudspeaker model's characteristics. A shorter simulation time may lead to a result dominated by transients and a longer simulation time makes the total simulation time excessively long.

To be able to evaluate how well the controllers perform, the uncontrolled loudspeaker has been used for comparison. In Figure 5.1 on the facing page, the THD of the uncontrolled model of the loudspeaker can be seen. From the figure it is clear that the level of THD is fairly stable and does not vary excessively with the different parameter values. This indicates that the loudspeaker model with perturbed parameter values generates a plausible output.

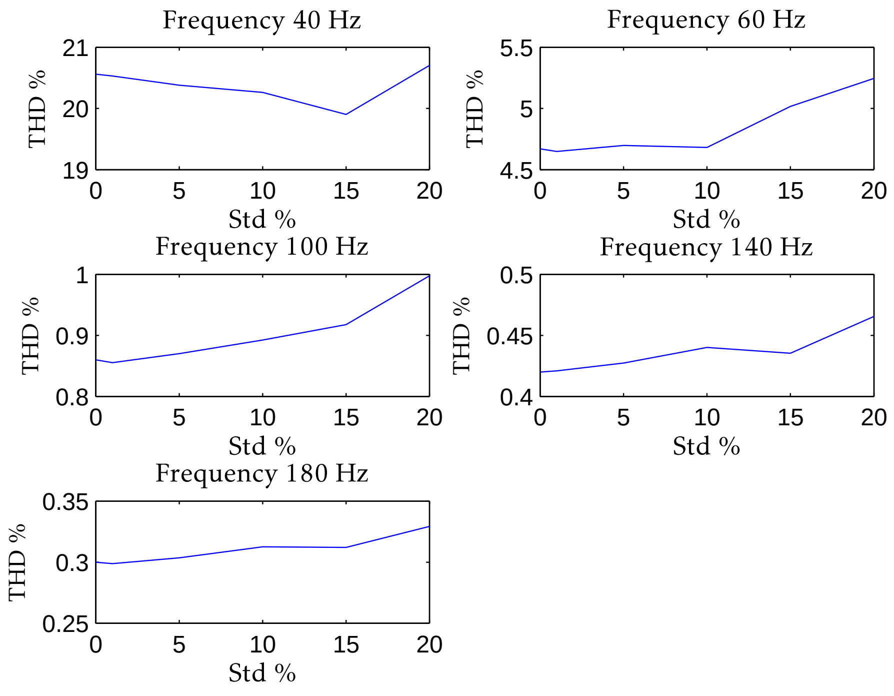

Figure 5.1: *Mean THD of the simulated uncontrolled loudspeaker with different parameter values. Note the scale difference.*

5.2 Feed-forward state estimation

During simulations using the feed-forward controller, the appearance of the system was as described in Section 4.2.1 on page 33 and the controller was based on exact input-output linearisation, described in Section 4.1 on page 29. To evaluate the linear dynamics derived in Chapter 4 versus the dynamics derived in Jakobsson and Larsson [2010], both designs have been simulated for equal sets of data.

The results of the simulations can be seen in Figure 5.2 on the next page where the controller design from Chapter 4 is marked 'New design' and the design from Jakobsson and Larsson [2010] is marked 'Old design'. The figure shows similar results for the different designs but the controller from Jakobsson and Larsson [2010] is slightly more sensitive to model errors. Therefore, the design from Chapter 4 will be used in the forthcoming simulations.

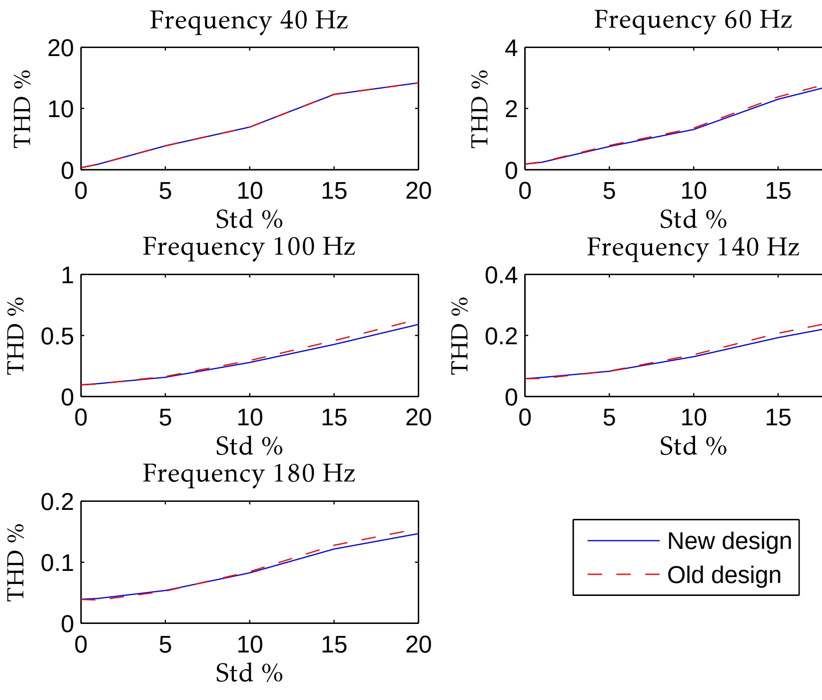

Figure 5.2: *Results from simulations of the feed-forward controller for two different pole placements. Note the scale difference.*

5.3 Observer-based state estimation

A couple of different observers have been evaluated, together with a controller based on exact input-output linearisation, to see if they are suitable for estimating the states of the loudspeaker. The observers were the first-order extended Kalman filter (EKF), second-order EKF (EKF2), unscented Kalman filter (UKF) and augmented UKF (AUKF). All filters except the first-order EKF managed to estimate the states properly in simulations. The first-order EKF caused several runs to crash, which is probably due to the fact that the EKF assumes that the second term in the Taylor expansion is small and can be neglected. For the crashing cases, the second-order term is probably too large and therefore the algorithm was not able to give proper estimates of the states.

A major issue when using these algorithms is their need of proper covariance matrices. These matrices have been tuned according to the remarks in Section 2.3 for a model without any added noise to its parameters.

As can be seen in Figure 5.3 on the facing page, the AUKF shows the best results for three out of five frequencies. For the two cases where EKF2 is superior, the

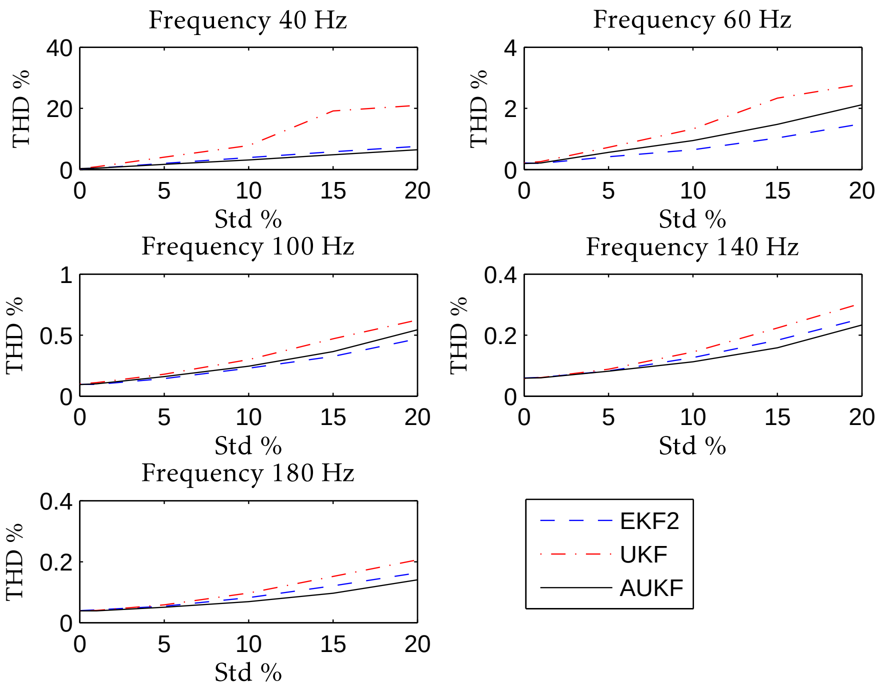

Figure 5.3: *Results from simulations with UKF, EKF2 and AUKF filters. Note the scale difference.*

frequency is close to the speaker's resonance frequency. This indicates that the second-order Taylor expansion, used by EKF2, catches the behaviour of the system more accurately for these frequencies than the sigma-point approach, used by AUKF.

In all simulations using observer-based controllers, the non-augmented UKF performs worst. Despite the result, this does not mean that the other filters need to perform better on a real system. In Sun et al. [2009] it is shown that UKF is scenario-dependent. They show that in presence of process noise with high variance, the UKF actually performs better than the AUKF. Because of that, it is still interesting to use the non-augmented UKF in real-life experiments.

Since all filters have static parameters, even though the deviation of the loudspeakers increases, it can be assumed that the THD at higher deviation could be decreased by adjusting the design parameters. This also means that when applying these filters on the real system, additional tuning may become necessary.

5.4 PID controller

As mentioned in Section 4.3, the PID controller is a cost-effective option to more complex strategies and can often give sufficient performance. The PID controller that has been used here was controlling the terminal current and hence the output signal from the controller had to be converted from current to voltage. This was done by using the impedance function with the approximation

$$sL_e \approx \frac{sL_e}{sL_e + 1} \tag{5.3}$$

to make the system proper. This approximation is a low-pass filter and will be valid for low frequencies.

To tune the parameters, the system was simulated for different parameter values and the total harmonic distortion was calculated for every case. The parameter values that rendered the lowest THD, was used in more extensive simulations. However, the results were either similar or slightly worse than the uncontrolled loudspeaker. That leads to the conclusion that a single PID controller, is not sufficient to compensate for the non-linearities regardless of its parameter values.

5.5 Feed-forward from reference with feedback

Since it is relatively inexpensive to measure current, the feed-forward state estimator was extended according to Section 4.4. To tune these PID parameters the same method as for the single PID controller was used.

Even though only the current was measured, Figure 5.4 on the next page shows that this clearly makes a difference. By knowing the value of a state, the feed-forward with feedback controller can adjust for the difference between measured and estimated current in contrast to the feed-forward controller which must assume that the model is correct. It can be seen in Figure 5.4 that this effect is larger when the deviation, from the real parameter grows. This is because when the deviation increases, the difference between the measured and estimated current grows as well.

At 60 Hz, the feed-forward with feedback controller is slightly worse than the controller solely using feed-forward state estimation. This indicates that the PID controller used for feedback is less well-tuned for the frequencies close to the resonance frequency at 65 Hz.

5.6 Comparison

For comparison reasons, the result for the best methods from each section can be seen in Figure 5.5 on page 48. As suspected, the state estimator without any

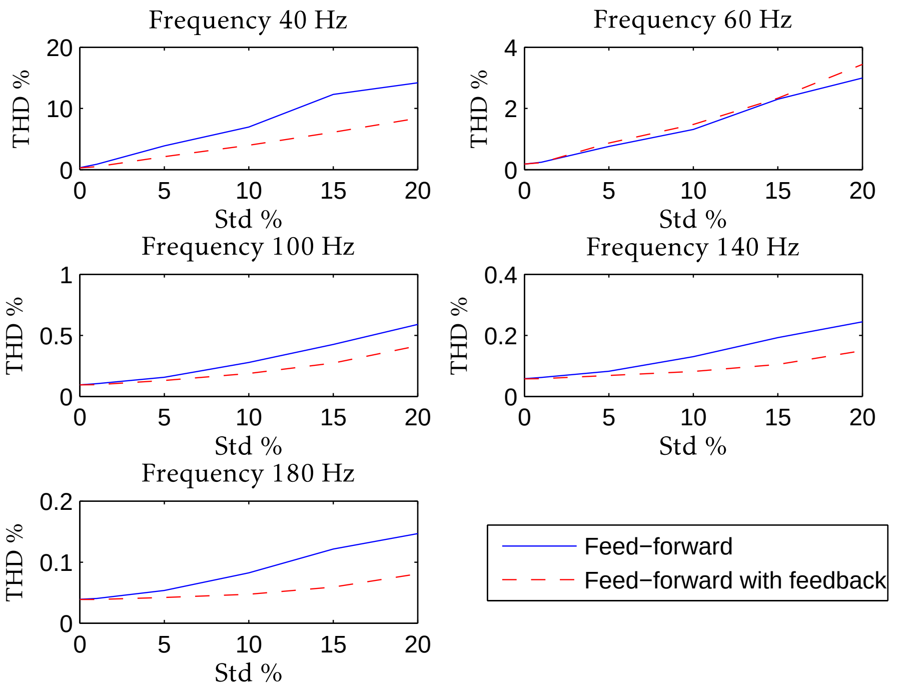

Figure 5.4: *Results from simulations with controllers based on feed-forward from reference with feedback and pure feed-forward controllers. Note the scale difference.*

feedback performs worse than the methods using feedback. Between the different approaches using feedback, it is either the AUKF or the feed-forward from reference with feedback algorithm that is best depending on frequency. It can also be seen that the derived control algorithms outperforms the uncontrolled loudspeaker significantly.

An important result found during the simulations was that the time to run each simulation was heavily dependent on the controller used. The feed-forward controller, which was also the simplest, took the shortest time to simulate and was ten times as fast as the more complex AUKF, which was the slowest. The controllers, from fastest to slowest to simulate were feed-forward, feed-forward with feedback, EKF2, UKF and AUKF.

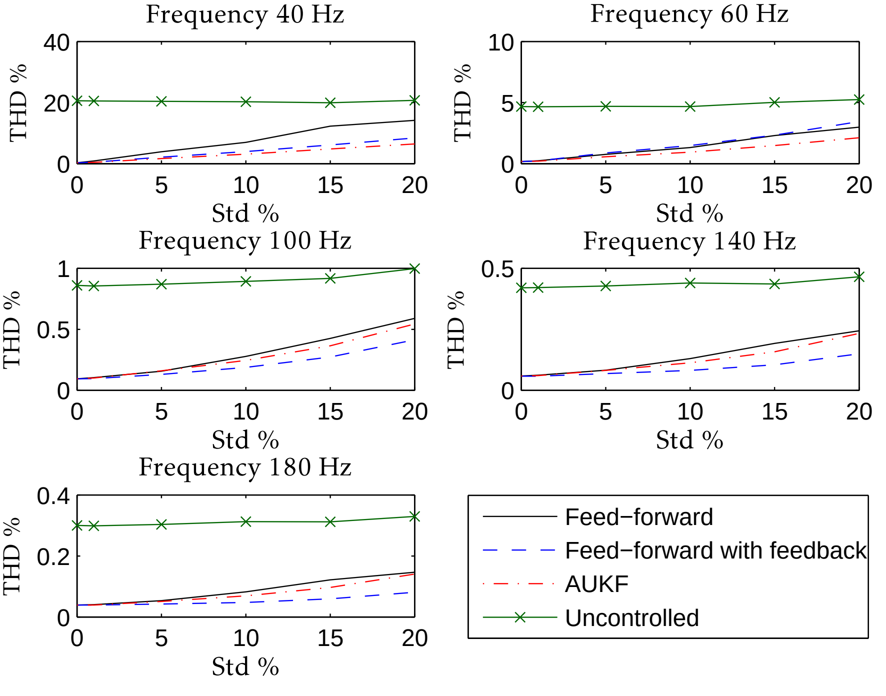

Figure 5.5: Comparison between simulations using the best control algorithms and the uncontrolled case. Note the scale difference.

6

Experiments

Some of the methods that were successful in the simulation environment have been implemented and evaluated in practice. This chapter covers all results from real-life experiments that have been performed, a brief description of the equipment that has been used and how the loudspeakers' parameters have been identified. To evaluate the algorithms' performance, the THD measure explained in (5.1) has been used.

6.1 Equipment

For the experiments, the equipment that has been supplied by Actiwave is an external sound card, a microphone, an amplifier unit and several Opalum-brand loudspeakers. The loudspeakers were of two different sizes, 4" and 5". The 4" speakers are of the same model as the loudspeaker used in Jakobsson and Larsson [2010]. Other necessary equipment, such as computers and measurement devices has been supplied by the automatic control division at the university. A picture of the test area can be seen in Figure 6.1 on the next page.

It should be noticed that, even though most of the distortion is created by the loudspeaker, a few percentages of THD are generated by the amplifier and the recording equipment. Exactly how much distortion the equipment will add depends on its settings, which were kept constant during all experiments.

In simulations, frequencies up to 180 Hz were used, while only frequencies up to 60 Hz were used during experiments. The reasons for this were hardware limitations and the fact that the experimental results showed no improvement above 60 Hz. For example, the levels of THD were almost identical for 60 and 100 Hz, regardless of the choice of the controller.

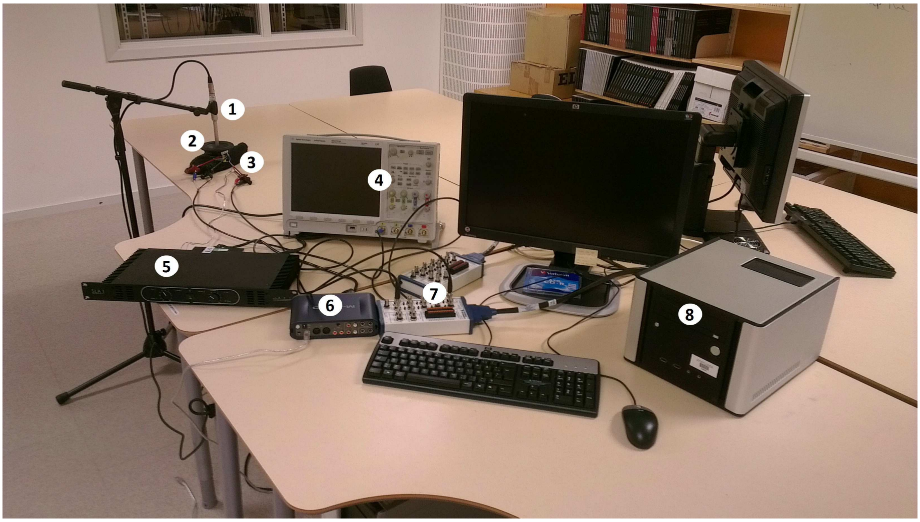

Figure 6.1: *Laboratory equipment overview. 1. Microphone, 2. Loudspeaker, 3. Stabilising woollen hat, 4. Oscilloscope, 5. AC amplifier, 6. Sound card, 7. Measurement devices, 8. xPC target computer.*

Even though the figures contain results for one specific 4" speaker, the results were similar when conducting experiments on the other 4" speaker and the 5" speakers. The major difference was that for the 5" speakers, the THD was attenuated for 20 Hz, while there was no improvement for 40 Hz and above.

6.2 AC amplifier compensation

During the experiments, an amplifier that was unable to amplify DC signals has been used. Since the controllers designed in Chapter 4 do not take that into account, some minor modifications have been made by introducing the amplifier model from Section 3.3. In Fränken et al. [2005] they approximate the AC amplifier transfer function from input voltage to output voltage, $G(s)$, as

$$G(s) = V_{amp} \cdot \frac{\alpha + s\tau}{1 + s\tau} \tag{6.1}$$

where α is a design parameter in the range $]0, 1[$. The parameter α should be tuned such that α/τ is slightly lower than the fundamental angular frequency of the signal. The variable u_{amp}, from Section 3.3, is introduced as a new state in the loudspeaker model which leads to recalculations of the exact input-output linearisation. Additionally, the input to the loudspeaker is now considered to be the amplifier output, e, rather than the control signal, u. Because of that, there is a need for monitoring the signal sent from the amplifier to the loudspeaker during experiments in order to tune the amplification constant V_{amp} properly.

Fränken et al. [2005] show that by using this approximation of the AC amplifier model in the controller, the voltage distortion in the amplifier will be compensated for and harmful zero-dynamics will be eliminated with the modified control law

$$u = u_{orig} + u_{amp}(1 - \alpha) \tag{6.2}$$

where u_{orig} is the control signal calculated according to (2.6).

6.3 Parameter identification

In order to compensate for the non-linearities of the loudspeaker, it is vital to have an accurate model. The loudspeaker model from Chapter 3 consists of several parameters that need to be accurately set in order to acquire a satisfying model. The values that need to be estimated are R_e, R_2, L_2, M, R_{ms} and the scaling of the non-linearities Bl, C_{ms}, L_e, compared to their measured values given by Klippel's measurement service. There are numerous approaches to this problem and the basics are described in Ljung and Glad [2009].

Basic knowledge about most of the parameter values was received by performing measurements according to Granqvist [2008], but there were still some parameters that needed to be estimated. To combine the estimations with the measurements, the measured parameter values were fed to the identification algorithms as initial guesses.

6.3.1 Impedance estimation

Due to lack of advanced measuring devices, all the loudspeaker model's parameter values could not be measured. Some of the parameters are even impossible to measure since they are merely physical representations rather than components. Instead, the parameters can be estimated by measuring the loudspeaker's impedance using a chirp signal and then match the model's impedance function, (3.18), to the measured data. This approach is called grey-box modelling because of its mixture between white-box modelling, where everything about the system is known, and black-box modelling, where nothing is assumed to be known.

In Figure 6.2 on the following page, a least-squares method in Matlab has been used to find the parameter values that generate the best possible fit between impedance model and measured impedance. The impedance profile looks legitimate since the impedance value for low frequencies and the resonance frequency are very plausible for the used loudspeaker model. The initial guess is the impedance received by using the parameter values from Jakobsson and Larsson [2010] and the measurable values by following Granqvist [2008]. As seen in the figure, despite the original dissimilarities with the measured impedance, the algorithm renders an accurate fit.

However, it is important to remember that the result in Figure 6.2 only gives a

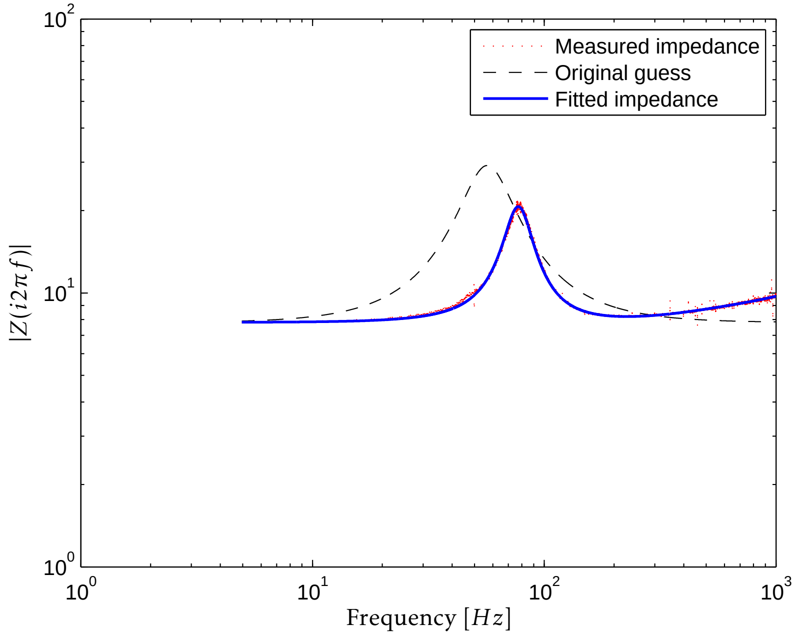

Figure 6.2: *Amplitude curves of measured, initially guessed and fitted impedance.*

set of parameters that generates a well-fitting impedance profile. Therefore, it is possible that the estimated parameters differ significantly from the real values.

6.3.2 Current estimation

Another grey-box modelling approach that has been utilised was to match the measured current with the modelled current. The model was the entire loudspeaker model with the terminal current as output. To receive a set of parameters, a prediction error estimation routine in Matlab's System Identification Toolbox has been used. By selecting the terminal current as output, the system's parameter values can be adjusted to generate an output as close as possible to the measured one.

To get a suitable measurement it is important to use an input signal that stimulates the desired parts of the loudspeaker model. Klippel and Schlechter [2010] recommend a sparse multi-tone sinusoid to catch the loudspeaker's dynamics at both higher and lower frequencies. They also state that it is important to use sine waves with frequencies such that the resonance frequency and the distortion from the non-linearities can be identified. By taking these recommendations into account, a sinusoidal signal with two fundamental frequencies, one at the resonance frequency and another slightly above, were used during these estimations.

This method is more computationally demanding than the impedance estimation method since it uses a non-linear numerical solver. On the other hand it could easily be extended to include multiple measurements such as cone displacement and velocity. This would probably improve the parameter estimation but requires more advanced measuring devices.

6.3.3 Comparison

When comparing the two parameter estimation algorithms they generate similar parameter values. Most of the parameters vary approximately 10-15% depending on the measurement data, initial values and frequencies used. However, the inductive parts of the loudspeaker represented by parameters L_e and L_2 have been recorded varying over 100% between runs.

It is also important to remark that some sets of estimated parameters for the 4" speakers are close to, but not exactly, the values measured by Klippel's measurement service in Jakobsson and Larsson [2010]. This indicates that the methods are able to generate valid sets of parameters.

An advantage of the current estimation method is that the non-linearities could be estimated as well if the cone displacement would be measured. The impedance approach is unable to perform such estimations since it is based upon a linearisation of the loudspeaker model.

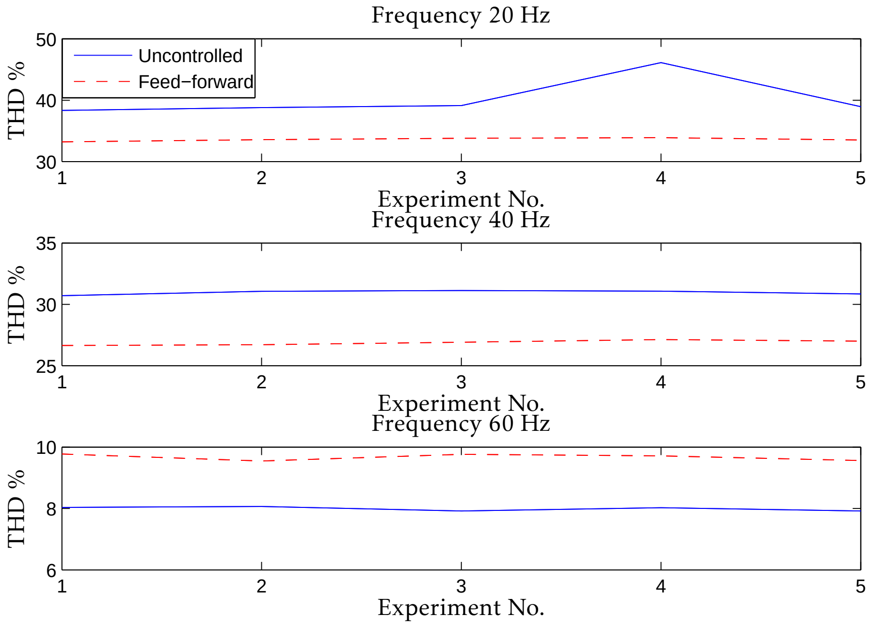

Figure 6.3: *Results from experiments using feed-forward state estimation compared to the uncontrolled case. Note the scale difference.*

6.4 Feed-forward state estimation

Several experiments have been performed with the controller and state estimator described in Section 4.2.1. The sample rate during these experiments was set constant to 44 100 Hz and the state estimator was working at the same rate. Results from testing one of the 4" speakers with parameter values estimated from the impedance profile can be seen in Figure 6.3 where the same experiment has been conducted five times. It is clear that the feed-forward algorithm decreases the THD for frequencies up to 40 Hz, but performs slightly worse for 60 Hz.

6.5 Observer-based state estimation

The observer-based approaches are the most computationally demanding methods used in this thesis. Therefore, several difficulties with implementing them on a real system have been encountered.

Both the ordinary UKF and the augmented one uses relatively simple calculations but for multiple sample points which increases the need of a fast processing unit. Due to the lack of processing power there were no success in implementing them to conduct experiments. The probable key to implementing these will be to utilise some sort of parallel processing unit, as a DSP or multi-core CPU.

The EKF2 uses, in contrast to the UKF, more computationally demanding operations, such as calculating Jacobians and Hessians. To be able to conduct experiments using EKF2, the sample rate had to be lowered to 14 700 Hz. The results when using the EKF2 were almost identical to the uncontrolled case, when using the same sample rate and for several values of the loudspeaker parameters for both speaker models. That parameter values have less impact than for the feed-forward cases indicates that the EKF2 is more robust to model errors. Even though no improvement of the THD was seen during these experiments it might be possible to achieve better performance by further tuning of the covariance matrices, especially considering the simulation results in Section 5.3.

6.6 Feed-forward from reference with feedback

Experiments with the controller from Section 4.4 has been conducted with a sample rate set constant to 44 100 Hz. Results from testing one of the 4" speakers with parameter values estimated from the impedance profile are presented in Figure 6.4 on the following page. It can be seen that the controller clearly improves the attenuation of the THD for frequencies up to 40 Hz, but at 60 Hz the THD is slightly increased. However, the THD may be possible to decrease even further by tuning of the PID parameters.

6.7 Comparison

A comparison between the results for the feed-forward controller with and without feedback can be found in Figure 6.5 on page 57. These results have been obtained for a 4" speaker with the same loudspeaker parameter values for both methods.

The controllers manage to decrease the level of THD for frequencies up to 40 Hz compared to the uncontrolled case, but is slightly worse for a signal at 60 Hz. In Figure 6.5, it can also be seen that the feed-forward controller using feedback outperforms the pure feed-forward controller for all measured frequencies.

To better see how the amplitudes of the harmonics change when using the controllers, Figure 6.6 on page 58 displays the amplitudes of the first six harmonics for different fundamental frequencies. It can be seen that the controllers manage to decrease the even-order harmonics, and especially the second, which is the biggest. The odd-order harmonics are almost untouched for the controller using feedback but slightly amplified when using the pure feed-forward controller. This indicates that the controllers manage to reduce the impact of symmetric parts of the non-linearities, but are less efficient in eliminating the asymmetric influence [Klippel, 2006].

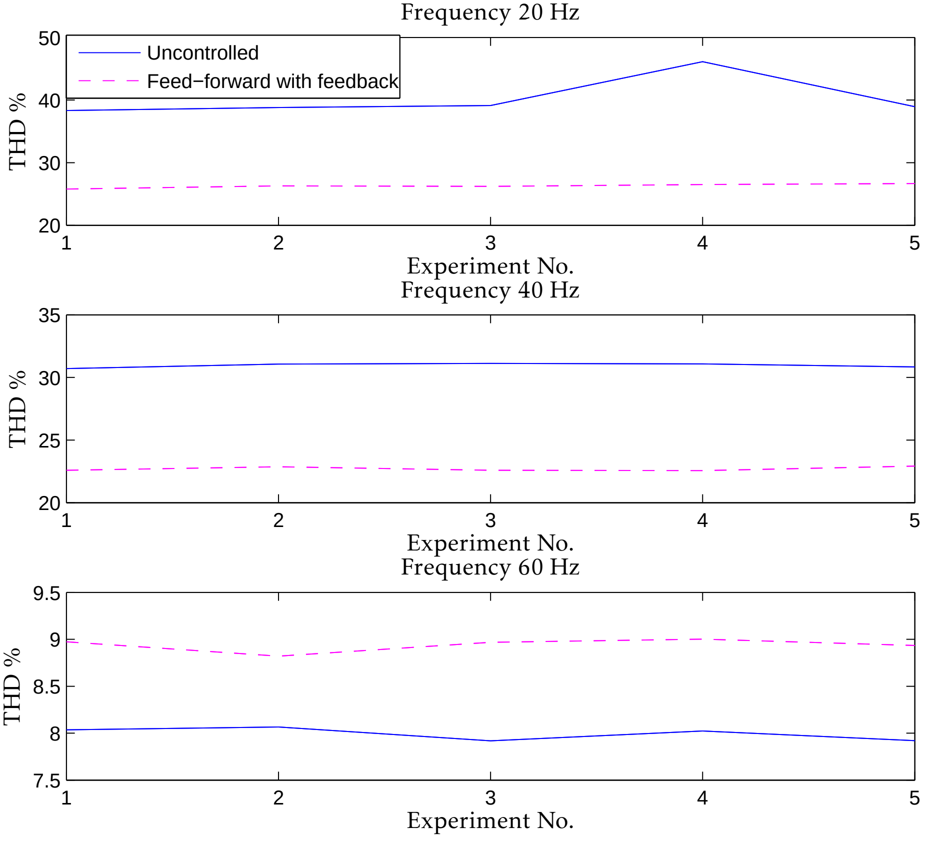

Figure 6.4: *Results from experiments using feed-forward with feedback control compared to the uncontrolled case. Note the scale difference.*

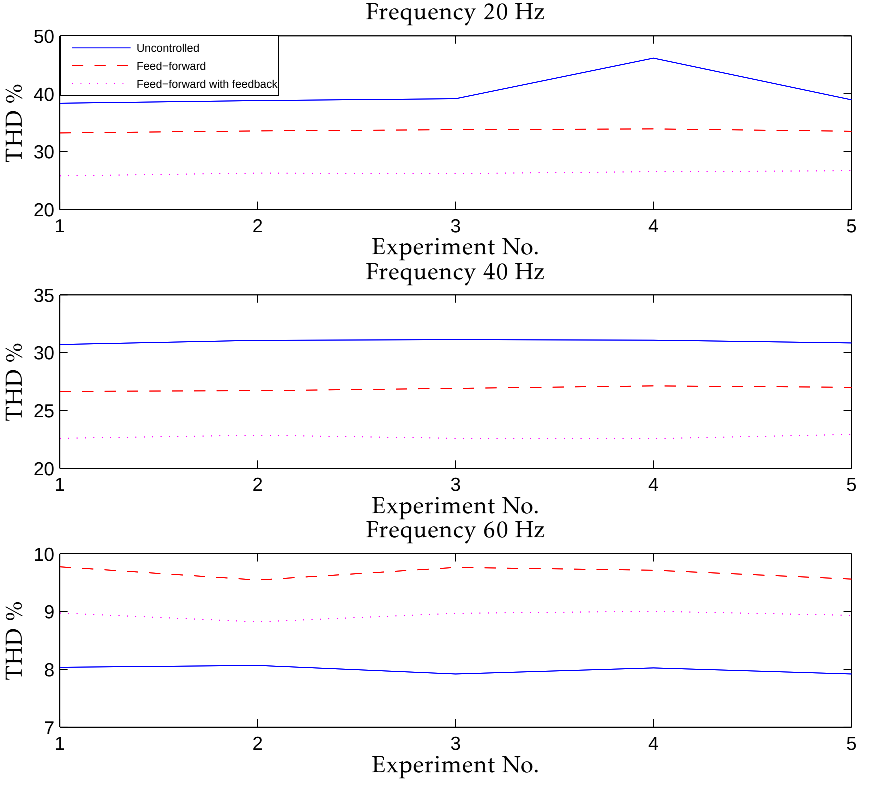

Figure 6.5: *Comparison between the feed-forward controller with and without feedback and the uncontrolled case. Note the scale difference.*

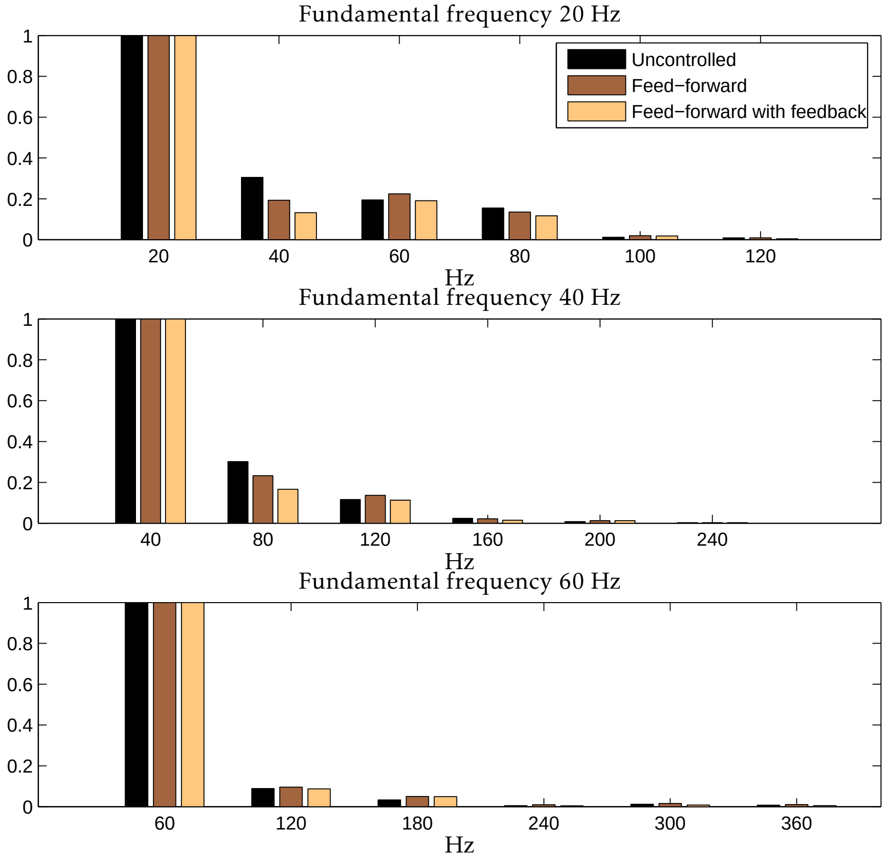

Figure 6.6: *Amplitudes of the harmonics, measured in portion of the amplitude of the fundamental frequency (first-order harmonic).*

Part IV

Discussion and Conclusions

7 Discussion

Before conclusions can be drawn it is important to analyse the results thoroughly. Especially, considering the difference between the results from simulations and experiments.

A major reason why the results from simulations are better than the ones from experiments is the inaccuracy of the used model. During simulations, the same model is used for both controlling and realising the loudspeaker. Even though their internal parameters were different in most of the simulations, there was no significant discrepancy. During experiments, the model could not possibly cover all the dynamics of a real-life loudspeaker and hence the results became worse.

One way to improve the results might be to modify the model that has been used. The model already consists of several non-linearities but, as mentioned in Chapter 3, the parameters R_2 and L_2 are mildly non-linear as well. By adding that fact it may be possible to achieve better compliance with the real loudspeaker. On the other hand, R_2 and L_2 are included in the model to improve the modelling of eddy currents at higher frequencies. Since the controller's main focus is at low frequencies these parameters will have little influence on the final result. Hence, it may be better to use the Thiele-Small model without R_2 and L_2 as a basis for new additions. This will eliminate the use of the state variable i_2 and hence make the model more manageable when adding new, more important, information.

A modification to the model that has been proven to positively alter the result was including the amplifier model. When Jakobsson and Larsson [2010] conducted experiments using the feed-forward controller they were unable to show any improvement when it comes to level of THD compared to the uncontrolled case. This is probably due to the fact that they used no compensation for the equipment they used. Therefore, it seems vital to analyse the equipment and compensate for possible harmful deformation of the control signal before the loudspeaker.

As mentioned in Chapter 6, several hardware issues were encountered and some algorithms could not even be implemented on the used hardware. One of the hardware limitations was that the measurement card could not produce output signals outside the range of ±10 Volts. This led to difficulties when trying to alter the amplitude of the input signal without disturbing the controller since it needs to properly calculate the signal that eventually will enter the loudspeaker. If the signal is distorted on the way, the state estimator will be predicting the next state values using a false amplitude of the loudspeaker input. To prevent this, the true voltage over the loudspeaker may be measured. A saturation could also be included in the controller to avoid this issue, but this needs further investigation since the control signal no longer will be the one calculated by the exact linearisation control law.

The controllers perform slightly worse than the uncontrolled case for higher frequencies in experiments. An approach to work around this issue would be to only have the controller active for frequencies lower than a desired threshold frequency. This might however not be a significant problem due to the fact that THD is automatically decreasing with higher frequencies and is vastly reduced for frequencies above the resonance frequency [Jakobsson and Larsson, 2010].

The difference between the controlled and uncontrolled case for higher frequencies is very small and may not be audible, even for audiophiles. According to Moscal [1994] it is not possible to perceive harmonic distortion lower than 1% at all, and differences less than a few percent is undetectable. Bareham [1989] also claims that tones with lower amplitude than -60 dB of the fundamental one will be impossible to detect. This indicates that the THD measure may be deceptive when including harmonics with very low amplitude. On the other hand, these harmonics will have very limited influence on the final THD value.

During the experiments, the controllers have performed better for the smaller-sized loudspeaker. It was even possible to use the same parameter values for the different speakers of the smaller model without any significant change in performance. The main difference between the larger and the smaller loudspeakers is probably due to the fact that the non-linearities are better suited for the smaller model since they were measured on such a loudspeaker using Klippel's measurement service in Jakobsson and Larsson [2010]. To adapt the non-linearities to the bigger type, the non-linear functions have been scaled by an estimated scaling factor but not skewed or changed in any other way. By measuring the non-linearities of the larger loudspeaker, the controllers will probably perform better.

8 Conclusions

Multiple controllers have been designed for attenuation of harmonic distortion. Several were successful during simulations using loudspeaker parameters measured by Klippel's measurement service. The first-order EKF was unable to properly estimate the loudspeaker's states, while a second-order EKF and both classes of UKF showed promising results.

Despite the promising simulation results, the original controllers were unable to show improvement in experiments due to the need of DC amplification. By including a simple model of the used AC amplifier, it was possible to achieve functional control for low frequencies during real-life experiments using a feed-forward controller. If feedback of the terminal current is used together with the feed-forward controller the THD can be reduced even further.

When using the designed controllers, it is important to use accurate loudspeaker parameter values. In simulations it is shown that the controllers perform worse for larger deviation of the parameter values. To receive accurate parameter values, two methods have been presented. The estimation method using impedance matching was able to generate sets of parameter values used in the controllers that showed improvements during experiments.

The second-order EKF was unable to show improvement during the experiments. The designed non-augmented and augmented UKF were not implemented due to hardware limitations.

9

Future work

The objective of this thesis was to continue the work of Jakobsson and Larsson [2010] in order to achieve a working controller. Even though controllers that attenuated the THD were derived, more work needs to be done before the methods are suitable for an industrial manufacturing.

9.1 Modelling

The loudspeaker model has been validated by Jakobsson and Larsson [2010], but may be reducible without any significant loss in performance. Since the controllers are working with signals with low frequencies it could be useful to investigate if the eddy current, i_2 , and its parameters, R_2 and L_2, generates any significant contribution to the controllers by using them in the loudspeaker model.

Another interesting point is to investigate which parameters make the largest difference, and thereby must be measured or estimated more accurately. Since it is known that some of the parameters have a temperature and ageing dependency [Pedersen, 2008], it could also be useful to look into how much this will influence the controllers and observers. It would also be beneficial to investigate the possibility to derive a parameter identification algorithm that adjusts the parameter values on-line in order to minimise THD. Such a method would probably need full state feedback, but should be able to supply accurate mappings of the non-linearities [Klippel, 2006].

Considering the AC amplifier's loss of ability to amplify DC components, it raises the question if compensation could be achieved in a different way than using a high-pass filter model. It would also be of interest to investigate if there are other components that disturb the signal to the speaker. To use these controllers in a loudspeaker that is manufactured for the consumer market, it might be necessary to modify the model, especially the loudspeaker box can heavily influence the behaviour of the speaker [Andersen, 2005].

9.2 Controller

Implementations of the UKFs were unsuccessful, in real-life experiments, due to lack of computational power. Therefore, it could be profitable to use hardware with better processing performance, or optimising the code to see if they would perform better than the second-order EKF.

Since the observers estimated the states well during simulations, it would be valuable to actually find out if the controllers using observers can reduce the THD by merely tuning the observers covariance matrices. There is also a possibility that the feed-forward with feedback controller can be improved by adjusting its PID parameters.

Bibliography

Martin Rune Andersen. Compensation of nonlinearities in transducers. Master's thesis, Technical University of Denmark, 2005. Cited on page 66.

Mingsian R. Bai and Chau-Min Huang. Expert diagnostic system for moving-coil loudspeakers using nonlinear modeling. *Acoustical Society of America 125*, 2009. Cited on page 20.

Glen M. Ballou. *Handbook For Sound Engineers*. Gulf Professional Publishing, 3 edition, 2005. Cited on page 5.

John R. Bareham. *Automatic Quality Testing of Loudspeaker Electroacoustic Performance*. Brüel & Kjær Application Note, 1989. Cited on page 62.

Mark A. Boer, Alex G. J. Nijmeijer, Hans Schurer, W. F. Druyvesteyn, Cornelis H. Slump, and Otto E. Hermann. Audibility of nonlinear distortion in loudspeakers. In *Audio Engineering Society Convention 104*, May 1998. URL `http://www.aes.org/e-lib/browse.cfm?elib=8462`. Cited on page 4.

Andrew Bright. *Active control of loudspeakers: An investigation of practical applications*. PhD thesis, Technical University of Denmark, 2002. Cited on pages 7 and 8.

Dietrich Fränken, Klaus Meerkötter, and Joachim Waßmuth. Observer-based feedback linearization of dynamic loudspeakers with AC amplifiers. *IEEE Transactions on Speech and Audio Processing*, 13(2):233 – 242, March 2005. Cited on pages 27, 50, and 51.

Torkel Glad and Lennart Ljung. *Reglerteknik: grundläggande teori*. Studentlitteratur, 4 edition, 2008. ISBN 978-91-44-02275-8. Cited on pages 9, 31, and 36.

Torkel Glad and Lennart Ljung. *Reglerteori: flervariabla och olinjära metoder*. Studentlitteratur, 2 edition, 2009. ISBN 978-91-44-03003-6. Cited on pages 9, 10, 11, 30, and 35.

Svante Granqvist. Mätning av högtalarelementets Thiele/Small-parametrar. Laboratory assignment in the course DT2420 at the Royal Institute of Technology, Sweden, 2008. URL `http://www.csc.kth.se/utbildning/kth/kurser/DT2420/`. Cited on page 51.

Fredrik Gustafsson. *Statistical sensor fusion*. Studentlitteratur, 1 edition, 2010. ISBN 978-91-44-05489-6. Cited on pages 11, 13, and 15.

R. Hirschorn. Invertibility of multivariable nonlinear control systems. *IEEE Transactions on Automatic Control*, 24(6):855 – 865, December 1979. ISSN 0018-9286. Cited on page 33.

David Jakobsson and Marcus Larsson. Modelling and compensation of nonlinear loudspeaker. Master's thesis, Chalmers tekniska högskola, 2010. Cited on pages 3, 5, 6, 19, 22, 23, 30, 31, 32, 35, 41, 42, 43, 49, 51, 53, 61, 62, and 65.

S. J. Julier and J. K. Uhlmann. Unscented filtering and nonlinear estimation. *Proceedings of the IEEE*, 92(3):401–422, 2004. Cited on page 13.

Rambabu Kandepu, Bjarne Foss, and Lars Imsland. Applying the unscented Kalman filter for nonlinear state estimation. *Journal of Process Control*, 18(7-8):753–768, 2008. Cited on pages 13 and 14.

Wolfgang Klippel. Nonlinear modeling of the heat transfer in loudspeakers. In *Audio Engineering Society Convention 114*, March 2003. URL `http://www.aes.org/e-lib/browse.cfm?elib=12535`. Cited on page 22.

Wolfgang Klippel. Tutorial: Loudspeaker nonlinearities - causes, parameters, symptoms. *Journal of the Audio Engineering Society*, 54(10), October 2006. Cited on pages 9, 55, and 65.

Wolfgang Klippel and Joachim Schlechter. Fast measurement of motor suspension nonlinearities in loudspeaker manufacturing. *Journal of the Audio Engineering Society*, 58(3):115–125, 2010. URL `http://www.aes.org/e-lib/browse.cfm?elib=15245`. Cited on page 53.

Lennart Ljung and Torkel Glad. *Modellbygge och simulering*. Studentlitteratur, 2 edition, 2009. ISBN 978-91-44-02443-1. Cited on page 51.

The Mathworks. *xPC Target 4: Getting started guide*, 6 edition, 2008. Cited on page 6.

Tony Moscal. *Sound Check: The Basics of Sound and Sound Systems*. Hal Leonard Corporation, 1994. Cited on page 62.

Karsten Øyen. Compensation of loudspeaker nonlinearities. Master's thesis, Norwegian University of Science and Technology, 2007. Cited on page 22.

Bo Rohde Pedersen. *Error correction of loudspeakers: A study of Loudspeaker Design supported by Digital Signal Processing*. PhD thesis, Aalborg University, 2008. ISBN 987-87-7606-024-4. Cited on pages 8 and 65.

Bo Rohde Pedersen and Finn T. Agerkvist. Nonlinear loudspeaker unit modeling. In *Audio Engineering Society Convention 125*, October 2008. URL `http://www.aes.org/e-lib/browse.cfm?elib=14752`. Cited on page 8.

Ulf Seidel and Wolfgang Klippel. Fast and accurate measurement of the linear transducer parameters. In *Audio Engineering Society Convention 110*, May 2001. URL `http://www.aes.org/e-lib/browse.cfm?elib=9988`. Cited on pages 25 and 36.

Jean-Jaques E. Slotine and Weiping Li. *Applied Nonlinear Control*. Prentice-Hall, Englewood Cliffs, New Jersey, 1991. ISBN 0-13-040890-5. Cited on pages 9 and 10.

Richard H. Small. Direct radiator loudspeaker system analysis. *Journal of the Audio Engineering Society*, 20(5):383–395, 1972. URL `http://www.aes.org/e-lib/browse.cfm?elib=2066`. Cited on page 19.

Fuming Sun, Guanglin Li, and Jingli Wang. Unscented Kalman filter using augmented state in the presence of additive noise. In *2009 IITA International Conference on Control, Automation and Systems Engineering*, 2009. Cited on pages 13, 15, and 45.

Neville Thiele. Loudspeakers in vented boxes: Part 1. *Journal of the Audio Engineering Society*, 19(5):382–392, 1971a. URL `http://www.aes.org/e-lib/browse.cfm?elib=2173`. Cited on page 19.

Neville Thiele. Loudspeakers in vented boxes: Part 2. *Journal of the Audio Engineering Society*, 19(6):471–483, 1971b. URL `http://www.aes.org/e-lib/browse.cfm?elib=2163`. Cited on page 19.

Yuanxin Wu, Dewen Hu, Meiping Wu, and Xiaoping Hu. Unscented Kalman filtering for additive noise case: Augmented vs. non-augmented. In *2005 American Control Conference*, June 2005. Cited on page 13.

Acta est fabula, plaudite!